SLAC-PUB-7652
May 1998

Massive Fermionic Corrections to the Heavy Quark Potential through Two Loops

Michael Melles

Stanford Linear Accelerator Center
Stanford University, Stanford, CA

and

University of Durham
Durham, United Kingdom

Submitted to *Physical Review D*

Stanford Linear Accelerator Center, Stanford University, Stanford, CA 94309

Work supported by Department of Energy contract DE–AC03–76SF00515.

hep-ph/9805216
SLAC-PUB 7652
DTP-98-18

Massive Fermionic Corrections to the Heavy Quark Potential Through Two Loops

Michael Melles [1]

Stanford Linear Accelerator Center
Stanford University, Stanford, CA

Abstract

A physically defined effective charge can incorporate quark masses analytically at the flavor thresholds. Therefore, no matching conditions are required for the evolution of the strong coupling constant through these thresholds. In this paper, we calculate the massive fermionic corrections to the heavy quark potential through two loops. The calculation uses a mixed approach of analytical, computer-algebraic and numerical tools including Monte Carlo integration of finite terms. Strong consistency checks are performed by ensuring the proper cancellation of all non-local divergences by the appropriate counterterms and by comparing with the massless limit. The size of the effect for the (gauge invariant) fermionic part of $\alpha_V(\mathbf{q}^2, m^2)$ relative to the massless case at the charm and bottom flavor thresholds is found to be of order 33%.

[1]Present address: University of Durham, UK; supported by Deutsche Forschungsgemeinschaft, Reference # Me 1543/1-1 and the European Union TMR-fund.

1 Introduction

In analogy to Quantum Electrodynamics, the heavy quark potential has been of interest in QCD from very early on [16, 34, 35, 41, 6, 1] as a model for the physical definition of the strong coupling constant [29]. Since it represents a potentially measurable quantity and gives naturally rise to a physical effective charge α_V [29], it is very interesting to study the QCD flavor thresholds in such a system [30] as the fermionic corrections are separately gauge invariant.

In the MS and the $\overline{MS}$ schemes, the running of the coupling constant, by construction, does not know about masses of quarks and since the couplings are non-physical, the Appelquist-Carazzone [33] decoupling theorem is not applicable. One has to turn to effective descriptions which match theories with m massless flavors onto a theory with $m-1$ massless and one massive flavor at the "heavy" quark threshold [42, 28, 15]. In this way, the dependence on the dimensional regularization mass parameter μ is reduced to next to leading order effects by giving up the analyticity of the coupling at the flavor threshold [40, 39, 37, 38, 14, 9].

While this procedure of matching conditions and effective descriptions is certainly workable, from a theoretical standpoint it would be advantageous to have a physical coupling constant definition which is analytic at thresholds. In addition, as a physical observable, the total derivative with respect to the renormalization scale μ vanishes. Such a system is given by identifying the ground state energy of the vacuum expectation value of the Wilson loop as the potential V between a static quark-antiquark pair in a color singlet state [16, 41, 21]:

$$V(r,m^2) = -\lim_{t\to\infty}\frac{1}{it} log\langle 0|Tr\,\{P\,exp\left(\oint dx_\mu A_a^\mu T^a\right)\}|0\rangle \tag{1}$$

where r denotes the relative distance between the heavy quarks, m the mass of "light" quarks contributing through loop effects and T^a the generators of the gauge group. It is then convenient to define the effective charge $\alpha_V(\mathbf{q}^2,m^2)$ as

$$V(\mathbf{q}^2,m^2) \equiv -\frac{4\pi C_F \alpha_V(\mathbf{q}^2,m^2)}{\mathbf{q}^2} \tag{2}$$

in momentum space. The factor C_F is the value of the Casimir operator T^aT^a in the fundamental representation of the external sources and factors out to all orders in perturbation theory. As one is free to choose the representation of the external particles, we obtain the static gluino potential by adopting the adjoint representation.

The massless case was recently calculated in Ref. [22] and in this paper, we will give all the two loop fermionic contributions to $\alpha_V(\mathbf{q}^2,m^2)$ for all perturbative values of the momentum transfer $\mathbf{q}^2 \equiv q_0^2 - q^2 = -q^2 > 0$ and for arbitrary values of the fermion mass m. In this context we are only interested in the two loop contributions to the potential in the effective Schroedinger equation for the heavy particles. This implies, for instance, that not always

the whole diagram contributes to the potential as certain parts can already be reproduced by the exponentiation of lower order diagrams. The necessity for this subtlety has its origin in the exponential present in Eq. 1. For a detailed discussion, see Ref. [41].

It is also important to note that the results of massive two loop integrals presented in this work are also relevant for the related problem of quark threshold production. For this application, though, it would be necessary to treat also the occurring imaginary parts of the integrals numerically as pole terms will contribute for timelike momentum transfers at the production threshold $q^2 = 4m^2$. A promising approach for this treatment might be the recently suggested Taylor expansion of integrands around threshold [18] by determining large and small scales in the problem. The heavy quark approximation eliminates the possibility of timelike momentum transfers in this work so that we do not need to worry about pole terms numerically. Nevertheless, we also list the contributions needed in this case for all integrals.

The paper is outlined as follows:

In section 2 we list all the occurring two loop contributions explicitly in the Feynman gauge and with the usage of heavy quark effective Feynman rules for the external sources. In section 3 the unrenormalized results for the two loop corrections are given in terms of two loop scalar integrals, for which explicit expressions are listed in appendix B. Section 4 contains all the required counterterms in the MS-renormalization scheme and it is shown that all non-local divergences cancel. The renormalization constants obtained are given explicitly and checked with the known results. Section 5 contains numerical results which demonstrate that the massless limit is obtained correctly and display the effect of including the mass terms for the charm and bottom flavor thresholds. In section 6 we make concluding remarks and indicate future lines of work with the presented results. Appendix A, finally, lists all the reductions from tensor to scalar integrals needed for the results displayed in section 3.

2 The Two Loop Corrections

In this section we present the non-Abelian contributions to the heavy quark potential that constitute the new results of this work. They are depicted in Fig. 2. The QED like diagrams, which need to be modified by their respective color factors, have been known for a long time [8] and can also be found in Refs. [14, 2, 3, 27] for instance. They are given here as well because we would like to be able to separate non-Abelian and Abelian contributions to the potential. It has been observed before [14] that their respective threshold behavior can be quite different. These diagrams, together with effectively "one loop" diagrams are given in Fig. 3. The weighted sum of all the graphs shown, modulo terms already generated by the exponentiation of the lower order Born and the one loop vacuum polarization diagram, give the complete gauge invariant fermionic corrections to the heavy quark potential

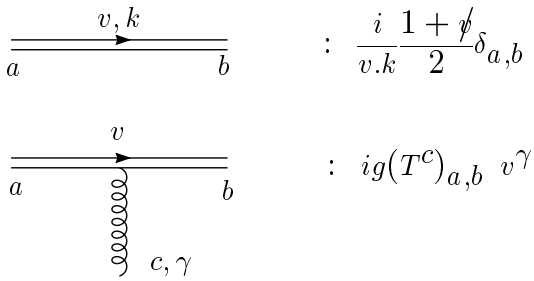

Figure 1: The Feynman rules for heavy quark effective theory used in this work for the source propagator and the source gluon vertex. For anti sources one has to make the replacement $v \longrightarrow -v$. The i-ε prescription is the same as for the usual fermion propagator.

at two loops in the Feynman gauge. The choice of this gauge simplifies the calculation because the decomposition into scalar two loop integrals is easier and it also reduces the three gluon vertex correction graph to zero in the heavy quark effective theory. Below we list all contributions at the two loop level. The abbreviations stand for $gse \equiv gluon\ self\ energy$, $vc \equiv vertex\ correction$, $cl \equiv crossed\ ladder$ and $olvc \equiv one\ loop\ vertex\ correction$. In the heavy quark limit we use the source gluon vertex and source propagator Feynman rules of heavy quark effective theory [19, 7] which are given in Fig. 1.

With these, and taking $v_\mu \equiv (1,0,0,0)$ and $q_0 = 0$ for the purely spacelike momentum transfer q, the two loop diagrams of Figs. 2 and 3 read in the Feynman gauge (summed over the external color degrees of freedom and including a symmetry factor of $\frac{1}{2}$ for the first three amplitudes):

$$\begin{aligned}
\mathcal{M}_{gse_1} &\equiv \frac{-ig^6\mu^{2\epsilon}}{q^4}\frac{C_F C_A T_F}{4}\delta^{\alpha,0}\delta^{\beta,0}\int\frac{d^nk}{(2\pi)^n}\int\frac{d^nl}{(2\pi)^n}\left[\frac{Tr\left\{\gamma^\delta\left(\not{v}-\not{k}+m\right)\gamma^\gamma\left(\not{v}+\not{q}+m\right)\gamma_\alpha\left(\not{v}+m\right)\right\}}{((l+q)^2-m^2)(l^2-m^2)((l-k)^2-m^2)(k+q)^2k^2}\right. \\
&\left.\times\left((q-k)_\gamma g_{\delta,\beta}+(-k-2q)_\delta g_{\gamma,\beta}+(2k+q)_\beta g_{\delta,\gamma}\right)\right] \qquad (3) \\
\mathcal{M}_{gse_2} &\equiv \frac{-ig^6\mu^{2\epsilon}}{q^4}\frac{C_F C_A T_F}{2}\delta^{\alpha,0}\delta^{\beta,0}\int\frac{d^nk}{(2\pi)^n}\int\frac{d^nl}{(2\pi)^n}\left[\frac{Tr\left\{\gamma^\gamma\left(\not{v}-\not{k}+m\right)\gamma^\delta\left(\not{v}+m\right)\right\}}{(l^2-m^2)((l-k)^2-m^2)(k+q)^2k^4}\right. \\
&\left.\times\left((-2q-k)_\gamma g_{\sigma,\alpha}+(-k+q)_\sigma g_{\gamma,\alpha}+(2k+q)_\alpha g_{\sigma,\gamma}\right)\left((q-k)_\sigma g_{\delta,\beta}+(-2q-k)_\delta g_{\sigma,\beta}+(2k+q)_\beta g_{\delta,\sigma}\right)\right] \qquad (4) \\
\mathcal{M}_{gse_3} &\equiv \frac{-ig^6\mu^{2\epsilon}}{q^4}\frac{C_F C_A T_F}{2}\delta^{\alpha,0}\delta^{\beta,0}\int\frac{d^nk}{(2\pi)^n}\int\frac{d^nl}{(2\pi)^n}\left[\frac{Tr\left\{\gamma^\gamma\left(\not{v}-\not{k}+m\right)\gamma^\delta\left(\not{v}+m\right)\right\}}{(l^2-m^2)((l-k)^2-m^2)k^4}\right. \\
&\left.\times\left(g_{\gamma,\beta}g_{\alpha,\delta}-2g_{\gamma,\delta}g_{\alpha,\beta}+g_{\gamma,\alpha}g_{\delta,\beta}\right)\right] \qquad (5)
\end{aligned}$$

$$\mathcal{M}_{gse_4} \equiv \frac{-ig^6\mu^{2\epsilon}}{q^4}\left(C_F^2-\frac{C_FC_A}{2}\right)T_F\,\delta^{\alpha,0}\delta^{\beta,0}\int\frac{d^nk}{(2\pi)^n}\int\frac{d^nl}{(2\pi)^n}$$
$$\times\left[\frac{Tr\left\{\gamma_\alpha\left(\not l+\not q+m\right)\gamma_\gamma\left(\not k+\not q+m\right)\gamma_\beta\left(\not k+m\right)\gamma^\gamma\left(\not l+m\right)\right\}}{((l+q)^2-m^2)(l^2-m^2)(l-k)^2((k+q)^2-m^2)(k^2-m^2)}\right] \quad (6)$$

$$\mathcal{M}_{gse_5} \equiv \frac{-ig^6\mu^{2\epsilon}}{q^4}C_F^2T_F\,\delta^{\alpha,0}\delta^{\beta,0}\int\frac{d^nk}{(2\pi)^n}\int\frac{d^nl}{(2\pi)^n}\left[\frac{Tr\left\{\gamma_\alpha\left(\not k+\not q+m\right)\gamma_\beta\left(\not k+m\right)\gamma_\gamma\left(\not l+m\right)\gamma^\gamma\left(\not k+m\right)\right\}}{(l^2-m^2)(l-k)^2((k+q)^2-m^2)(k^2-m^2)^2}\right] \quad (7)$$

$$\mathcal{M}_{vc_1} \equiv \frac{ig^6\mu^{2\epsilon}}{q^2}\frac{C_FC_AT_F}{2}\delta^{\alpha,0}\delta^{\beta,0}\delta^{\gamma,0}\int\frac{d^nk}{(2\pi)^n}\int\frac{d^nl}{(2\pi)^n}\frac{Tr\left\{\gamma_\gamma\left(\not l-\not k+m\right)\gamma_\alpha\left(\not l+\not q+m\right)\gamma_\beta\left(\not l+m\right)\right\}}{((l+q)^2-m^2)(l^2-m^2)((l-k)^2-m^2)(k+q)^2k^2k_0} \quad (8)$$

$$\mathcal{M}_{vc_2} \equiv \frac{ig^6\mu^{2\epsilon}}{q^2}\frac{C_FC_AT_F}{2}\delta^{\alpha,0}\delta^{\beta,0}\delta^{\gamma,0}\int\frac{d^nk}{(2\pi)^n}\int\frac{d^nl}{(2\pi)^n}\left[\frac{Tr\left\{\gamma_\alpha\left(\not l-\not k+m\right)\gamma_\nu\left(\not l+m\right)\right\}}{(l^2-m^2)((l-k)^2-m^2)(k+q)^2k^4k_0}\right.$$
$$\left.\times\left((q-k)_\beta g_{\nu,\gamma}+(-k-2q)_\nu g_{\beta,\gamma}+(2k+q)_\gamma g_{\nu,\beta}\right)\right] \quad (9)$$

$$\mathcal{M}_{vc_3} \equiv \frac{ig^6\mu^{2\epsilon}}{q^2}\frac{C_FC_AT_F}{2}\delta^{\alpha,0}\delta^{\beta,0}\int\frac{d^nk}{(2\pi)^n}\int\frac{d^nl}{(2\pi)^n}\frac{Tr\left\{\gamma_\alpha\left(\not l-\not k+m\right)\gamma_\beta\left(\not l+m\right)\right\}}{(l^2-m^2)((l-k)^2-m^2)k^4(k_0+i\varepsilon)^2} \quad (10)$$

$$\mathcal{M}_{cl} \equiv -ig^6\mu^{2\epsilon}\frac{C_FC_AT_F}{2}\delta^{\alpha,0}\delta^{\beta,0}\int\frac{d^nk}{(2\pi)^n}\int\frac{d^nl}{(2\pi)^n}\frac{Tr\left\{\gamma_\alpha\left(\not l-\not k+m\right)\gamma_\beta\left(\not l+m\right)\right\}}{(l^2-m^2)((l-k)^2-m^2)k^4(k+q)^2(k_0+i\varepsilon)^2} \quad (11)$$

$$\mathcal{M}_{olvc} \equiv \frac{ig^6\mu^{2\epsilon}}{q^4}\frac{C_FC_AT_F}{2}\delta^{\alpha,0}\delta^{\beta,0}\int\frac{d^nl}{(2\pi)^n}\frac{Tr\left\{\gamma_\alpha\left(\not l-\not q+m\right)\gamma_\beta\left(\not l+m\right)\right\}}{(l^2-m^2)((l-q)^2-m^2)}\int\frac{d^nk}{(2\pi)^n}\frac{1}{k^2(k_0+i\varepsilon)^2} \quad (12)$$

It should be noted that in our case there is no need for an i-ε prescription in the denominators of Eqs. 3 through 9 as the spacelike nature of the physical momentum transfer only leads to purely real integrals and no unambiguous pole terms occur in the denominators of those diagrams. This feature also simplifies the Monte Carlo integration of the finite parts of the contributing graphs. The three graphs 10, 11 and 12 display infra-red divergences which cancel in the sum. The one loop vertex correction graph $\mathcal{M}_{olvc}$ vanishes in dimensional regularization, however, is needed to ensure the proper cancellation of infra-red divergences.

The color factors given are not always the full color factors. Only those contributing to the potential are listed. The Casimir invariants [23] for a general $SU(N)$ group are defined by

$$C_A \equiv N \quad , \quad C_F \equiv \frac{N^2-1}{2N} \quad (13)$$

Furthermore, $Tr\{T^aT^b\} \equiv T_f\delta^{a,b} = \frac{1}{2}\delta^{a,b}$. The color factor for $\mathcal{M}_{vc_1}$ includes the sum of the graph shown in Fig. 2 plus the term stemming from the fermion momenta reversed contribution. Only the sum is proportional to C_A, the other terms vanish according to Furry's theorem, as is the case in QED. For QCD, the crossed ladder diagrams do contribute as they contain a color factor proportional to $C_F^2-\frac{C_FC_A}{2}$, whereas the straight ladder graph has a color factor proportional to C_F^2 only. This will be expounded on in section 3.1. In QED, the sum

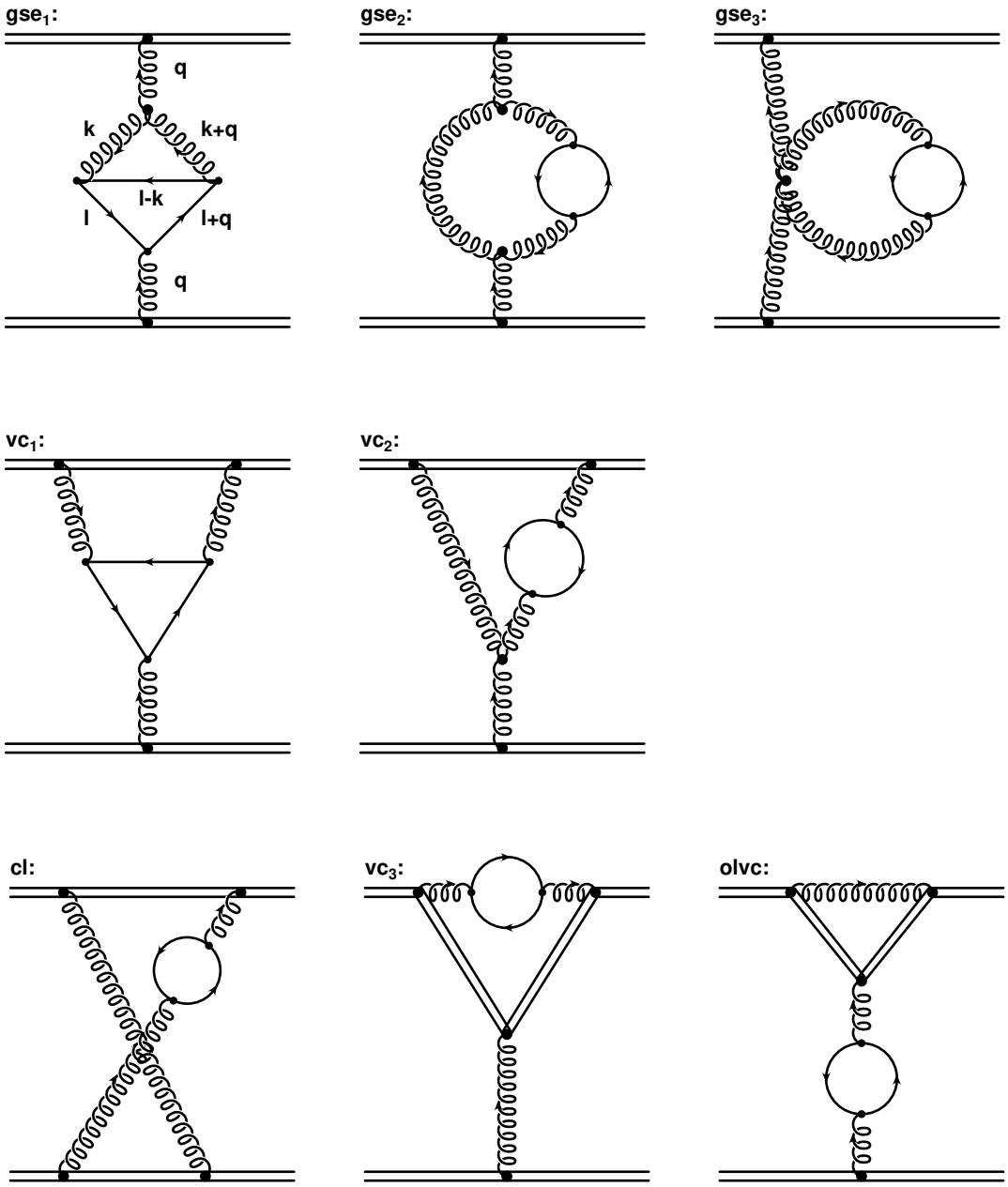

Figure 2: The non-Abelian Feynman diagrams contributing to the massive fermionic corrections to the heavy quark potential at the two loop level. The first two rows contain diagrams with a typical non-Abelian topology. Double lines denote the heavy quarks, single lines the "light" quarks. Color and Lorentz indices are suppressed in the first graph. The notation for the remaining digrams is analogous. The last line includes the infra-red divergent "Abelian" Feynman diagrams. While the topology of these three diagrams is the same as in QED, they contribute to the potential only in the non-Abelian theory due to color factors $C_F C_A$. In addition, although each diagram is infra-red divergent, their sum is infra-red finite.

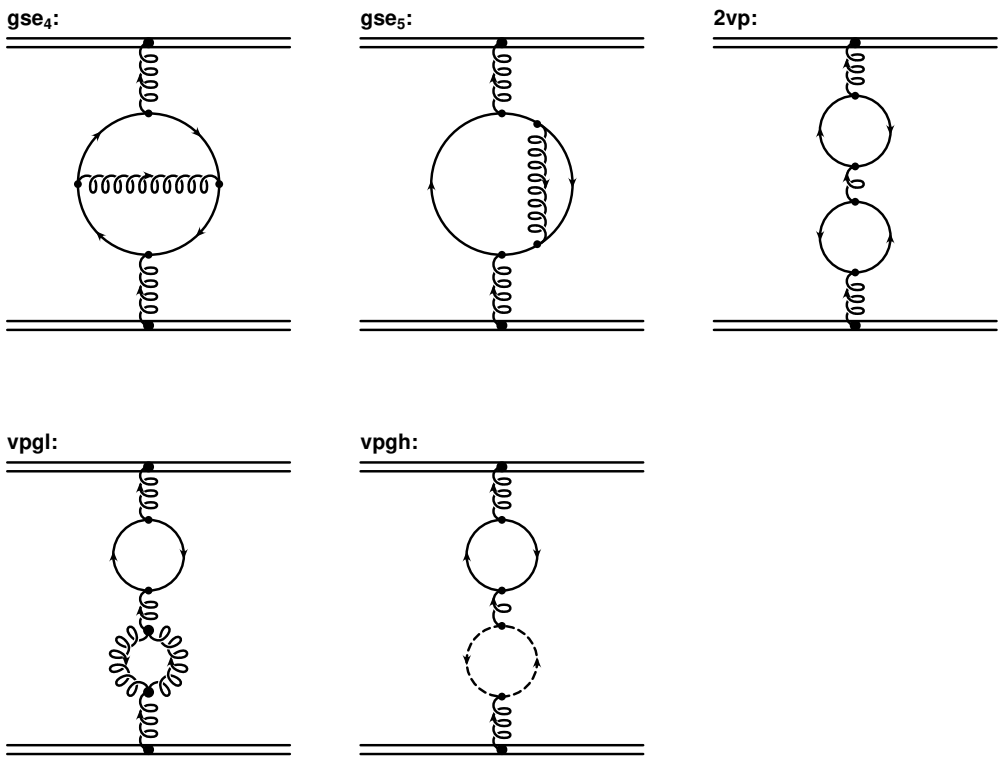

Figure 3: The infra-red finite Feynman diagrams with an Abelian topology (upper line) contributing to the massive fermionic corrections to the heavy quark potential at the two loop level plus diagrams consisting of one loop insertions with non-Abelian terms (lower line).

of all vertex, ladder and crossed ladder Feynman diagrams are equivalent to the iteration of the potential in the Schroedinger theory. $\alpha_{V_{QED}}$ and the effective coupling [5] differ, therefore, only at three loops due to light by light scattering contributions.

3 Unrenormalized Results

The two loop integrals needed for the expressions of Eqs. 3 through 9 are treated in separate ways in this work depending on whether or not they contain two or more internal fermion lines. In the former case we integrate the fermion loop first as will be explained below. For the vertex correction contribution $\mathcal{M}_{vc_1}$ we integrate the fermion loop analytically as well with all the Lorentz indices projected to zero and then proceed with additional Feynman parameters for the remaining loop integration.

The two point functions $\mathcal{M}_{gse_1}$, $\mathcal{M}_{gse_4}$ and $\mathcal{M}_{gse_5}$ are treated in a completely different manner as the above techniques would now be too cumbersome. We project the complicated tensor structure onto scalar quantities as described below and then proceed with an algebraic reduction into scalar two loop integrals. This reduction

is programmed in FORM [13] and details are presented in appendix A. The resulting scalar integrals are then evaluated by employing standard Feynman parameter techniques and explicit results are listed in appendix B. Overall results for the various amplitudes are obtained by expanding the n-dimensional results around $\epsilon = 0$ with MAPLE. It is important to notice, given the complexity of the calculation, that the translation into FORTRAN code was also performed by MAPLE, thus dramatically reducing the chance of accidental mistakes. The evaluation of finite parts is done with the Monte Carlo integrator VEGAS [25].

For the two point functions we use the following decomposition into transverse (t) and longitudinal (l) components:

$$\Pi_{\alpha,\beta}\left(q\right) \equiv \left(g_{\alpha,\beta} - \frac{q_\alpha q_\beta}{q^2}\right)\Pi_t\left(q^2\right) + \frac{q_\alpha q_\beta}{q^2}\Pi_l\left(q^2\right) \tag{14}$$

from which it follows that in $n = 4 - \epsilon$ dimensions

$$\Pi_t\left(q^2\right) = \frac{1}{n-1}\left(g^{\alpha,\beta} - \frac{q^\alpha q^\beta}{q^2}\right)\Pi_{\alpha,\beta}\left(q\right) \tag{15}$$

$$\Pi_l\left(q^2\right) = \frac{q^\alpha q^\beta}{q^2}\Pi_{\alpha,\beta}\left(q\right) \tag{16}$$

With this notation and the heavy quark effective Feynman rules depicted in Fig. 1 we arrive at

$$\mathcal{M}_{gse_i} \equiv \frac{g^2 C_F}{q^4}\delta^{\alpha,0}\delta^{\beta,0}\Pi^i_{\alpha,\beta}\left(q\right) \quad , \; i = \{1...5\} \tag{17}$$

The result of the decomposition for the transverse component of the gluon self energy graph $\mathcal{M}_{gse_1}$, using the relations given in appendix A, reads

$$\begin{aligned}
\Pi^1_t = {} & \frac{ig^4 C_A T_F}{4(n-1)}\left[\left(n\frac{8}{3} - \frac{20}{3}\right)\left(A_2 B_{12'} - m^2 T_{12'35}\right) + (4n-10)\,T_{235} + (8-4n)\,A_2 B_{12} + \left(n\frac{8}{3} - \frac{14}{3}\right)T_{135}\right. \\
& +16\left(q^2 - q^2\frac{n}{2} - m^2\right)T_{1235} + q^2\,(4n-6)\,T_{2345} + q^2\,(2n-4)\,B_{12}B_{45} - 8q^2 m^2 T_{12345} + 8A_2 B_{45} \\
& +\frac{m^2}{q^2}\left\{\left(n\frac{8}{3} - \frac{20}{3}\right)\left(m^2 T_{12'35} + T_{2'35} - A_2 B_{12'} + \frac{1}{m^2}A_2^2\right) + 16T_{235} - \left(n\frac{8}{3}\right.\right. \\
& \left.\left. + \frac{28}{3}\right)T_{135}\right\} + \frac{1}{n-1}\left\{-n\frac{2}{3}m^2 T_{12'35} + nT_{235} - n\frac{7}{3}T_{135} - 4nA_2 B_{45} + n\frac{2}{3}A_2 B_{12'} - 8m^2 T_{2345}\right. \\
& -4m^2 T_{2355} + 4T_{135} + q^2\left(4m^2 T_{23455} + (4-2n)A_2 C_{455} - nT_{2345}\right) + \frac{1}{q^2}\left(4m^2\left(T_{135} - T_{235}\right)\right. \\
& \left.\left.\left. +n\frac{2}{3}\left(m^4 T_{12'35} - m^2 T_{135} + m^2 T_{2'35} - m^2 A_2 B_{12'} + A_2^2\right)\right)\right\}\Bigg]
\end{aligned} \tag{18}$$

It is also useful to examine the $m \longrightarrow 0$ limit of the above expression as this case was calculated in Ref. [21] and can serve a valuable test for the above expression. By inspecting the occurring integrals we find the massless limit to correspond to

$$\begin{aligned}\Pi^1_{t_{m\longrightarrow 0}} &= \frac{ig^4 C_A T_F}{4(n-1)}\left[\left(n\frac{8}{3}-\frac{n}{n-1}\frac{7}{3}-\frac{14}{3}+\frac{4}{n-1}\right)T_{135}+16\left(q^2-q^2\frac{n}{2}\right)T_{1235}+q^2\left(2n-4\right)B_{12}B_{45}\right.\\ &\left.+q^2\left(4n-6-\frac{n}{n-1}\right)T_{2345}\right] \end{aligned} \tag{19}$$

These terms are also, as expected, the only ones contributing to the gluon wave function renormalization constant. In other words, all divergent parts of the two and one loop integrals which vanish in the massless limit in the expression 18 add up to zero identically. This in itself is an important check of the overall expression. In the heavy quark limit we can neglect the timelike component of the four momentum transfer q, i.e. $q_0 = 0$ as was already mentioned before. This means that we do not need the longitudinal component of $\mathcal{M}_{gse_1}$, however, we list it here for completeness:

$$\begin{aligned}\Pi^1_l &= \frac{ig^4 C_A T_F}{4}\left(\left(n\frac{8}{3}-\frac{20}{3}\right)\left(m^2 T_{12'35}-A_2 B_{12'}+\frac{1}{2}T_{135}\right)+2T_{235}-8A_2B_{45}-2q^2T_{2345}\right.\\ &+\frac{m^2}{q^2}\left\{\left(n\frac{8}{3}-\frac{20}{3}\right)\left(A_2B_{12'}-\frac{1}{m^2}A_2^2-T_{2'35}-m^2T_{12'35}\right)+\left(n\frac{8}{3}+\frac{28}{3}\right)T_{135}-16T_{235}\right\}\\ &+\frac{1}{n-1}\left[n\frac{2}{3}m^2T_{12'35}-nT_{235}+n\frac{7}{3}T_{135}+4nA_2B_{45}-n\frac{2}{3}A_2B_{12'}+8m^2T_{2345}+4m^2T_{2355}-4T_{135}\right.\\ &+q^2\left(nT_{2345}+2nA_2C_{455}-4m^2T_{23455}-4A_2C_{455}\right)+\frac{1}{q^2}\left\{4m^2\left(T_{235}-T_{135}\right)\right.\\ &\left.\left.\left.-\,n\frac{2}{3}\left(m^4T_{12'35}-m^2T_{135}+m^2T_{2'35}-m^2A_2B_{12'}+A_2^2\right)\right\}\right]\right)\end{aligned} \tag{20}$$

A good check on the consistency of the employed decomposition is given by the absence of infra-red divergences. None of the two point amplitudes in this work is infra-red divergent to begin with, however, in intermediate steps of the calculation those do occur. An example is given above by the two integrals T_{2355} and T_{23455} for which only the combination $q^2T_{23455} - T_{2355}$ is infra-red finite and this is how they enter into Eqs. 18 and 20. The function A_2C_{455} only seems to have an infra-red divergence, however, in dimensional regularization it can actually be written as an ultra-violet divergence. This is done in appendix B.

For the two diagrams that have an Abelian topology, Eqs. 6 and 7, we also give explicit results as usually only their sum is given in the literature [14, 10]. Here, however, we need both contributions separately due to the different color factors. In addition, Abelian and non-Abelian terms are separately gauge invariant and might display a different threshold behavior [14]. We find:

$$\Pi_t^4 = \frac{ig^4(C_F-\frac{C_A}{2})T_F}{(n-1)}\left[\left(n\frac{8}{3}-\frac{16}{3}\right)\left(A_2B_{12'}-m^2T_{12'35}\right)+\left(q^2\left((4n-8)q^2+(32-8n)m^2\right)-32m^4\right)T^A_{12345}\right.$$
$$+(8n-16)\left(T_{235}-A_2B_{12}\right)+32\left(q^2-q^2\frac{n}{2}-m^2\right)T_{1235}+\left(4n^2-n\frac{76}{3}+\frac{104}{3}\right)T_{135}$$
$$+\left(q^2\left(18n-2n^2-28\right)+16m^2\right)B_{12}B_{12}+\frac{1}{q^2}\left(\frac{8}{3}n\left(m^4T_{12'35}-m^2T_{135}+m^2T_{2'35}-m^2A_2B_{12'}+A_2^2\right)\right.$$
$$\left.\left.+16m^2\left(T_{235}-T_{135}\right)-\frac{16}{3}\left(m^4T_{12'35}-m^2T_{135}+m^2T_{2'35}-m^2A_2B_{12'}+A_2^2\right)\right)\right] \quad (21)$$

and for the longitudinal component:

$$\Pi_l^4 = ig^4(C_F-\frac{C_A}{2})T_F\left[\left(n\frac{8}{3}-\frac{16}{3}\right)\left(m^2T_{12'35}+\frac{1}{2}T_{135}-A_2B_{12'}\right)\right.$$
$$+\frac{1}{q^2}\left(\frac{16}{3}\left(m^4T_{12'35}-m^2T_{135}+m^2T_{2'35}-m^2A_2B_{12'}+A_2^2\right)\right.$$
$$\left.\left.+16m^2\left(T_{135}-T_{235}\right)-\frac{8}{3}n\left(m^4T_{12'35}-m^2T_{135}+m^2T_{2'35}-m^2A_2B_{12'}+A_2^2\right)\right)\right] \quad (22)$$

Similarly, for Eq. 7 we get the following result:

$$\Pi_t^5 = \frac{ig^4C_FT_F}{(n-1)}\left[\left(n^2-n\frac{16}{3}-\frac{20}{3}\right)\left(A_2B_{12'}-m^2T_{12'35}\right)-16m^2T_{1235}+\left((16-8n)q^2m^2-32m^4\right)T_{12235}\right.$$
$$+\left(n^2-4n+4\right)\left(q^2T_{12'35}-T_{2'35}+2A_2B_{22}-A_2B_{22'}+q^2A_2C_{122'}-2q^2A_2C_{122}\right)-\left(n^2-\frac{14}{3}n+\frac{16}{3}\right)T_{135}$$
$$+m^2\left(8n-16\right)\left(T_{2235}-A_2C_{122}\right)-\frac{1}{q^2}\left(\frac{4}{3}n\left(m^4T_{12'35}-m^2T_{135}+m^2T_{2'35}-m^2A_2B_{12'}+A_2^2\right)\right.$$
$$\left.\left.+8m^2\left(T_{235}-T_{135}\right)-\frac{8}{3}\left(m^4T_{12'35}-m^2T_{135}+m^2T_{2'35}-m^2A_2B_{12'}+A_2^2\right)\right)\right] \quad (23)$$

and for the longitudinal component:

$$\Pi_l^5 = -ig^4C_FT_F\left[\left(n\frac{4}{3}-\frac{8}{3}\right)\left(m^2T_{12'35}+\frac{1}{2}T_{135}-A_2B_{12'}\right)\right.$$
$$+\frac{1}{q^2}\left(\frac{8}{3}\left(m^4T_{12'35}-m^2T_{135}+m^2T_{2'35}-m^2A_2B_{12'}+A_2^2\right)\right.$$
$$\left.\left.+8m^2\left(T_{135}-T_{235}\right)-\frac{4}{3}n\left(m^4T_{12'35}-m^2T_{135}+m^2T_{2'35}-m^2A_2B_{12'}+A_2^2\right)\right)\right] \quad (24)$$

It can easily be seen that both parts of the two functions in Eqs. 21 and 23 multiplying $\frac{1}{q^2}$ are identical up to a minus sign when 23 is multiplied by the multiplicity factor 2. This is required by the gauge structure of the gluon propagator. Also their longitudinal parts add up to zero for the terms proportional to C_F only. This just

checks the well known properties of the Abelian theory. It does not hold for the C_A parts of Eqs. 18 and 21 as they would get modified by the additional diagrams. These, however, were calculated in this work without the above reduction scheme as follows:

We use the result of the integrated fermion loop which reads (omitting color and coupling constant factors) [32]:

$$\pi_{\mu,\nu}(k,m) \equiv \mu^\epsilon \int \frac{d^n l}{(2\pi)^n} \frac{Tr\{\gamma_\mu (\not{l} - \not{k} + m) \gamma_\nu (\not{l} + m)\}}{(l^2 - m^2)((l-k)^2 - m^2)} \equiv \left(k^2 g_{\mu,\nu} - k_\mu k_\nu\right) \pi(k^2, m^2) \tag{25}$$

with

$$\pi(k^2, m^2) = \frac{i(-)^{\frac{n}{2}} \eta^{\frac{\epsilon}{2}}}{(4\pi)^2} \Gamma\left(\frac{\epsilon}{2}\right) \int_0^1 dx \frac{8x(1-x)}{\left(\frac{k^2}{m^2} x(1-x) - 1\right)^{\frac{\epsilon}{2}}} \tag{26}$$

where η is given in Eq. 85. For completeness, we also list the sum of the gluon and ghost contributions in the Feynman gauge [17, 36] to the gluon propagator:

$$\pi_{\mu,\nu}(q) \equiv \left(q^2 g_{\mu,\nu} - q_\mu q_\nu\right) \pi(q^2) = \left(q^2 g_{\mu,\nu} - q_\mu q_\nu\right) \frac{i\zeta^{\frac{\epsilon}{2}} \Gamma\left(\frac{\epsilon}{2}\right) \Gamma\left(2 - \frac{\epsilon}{2}\right)^2 \left(5 - \frac{3\epsilon}{2}\right)}{8\pi^2 \Gamma(4-\epsilon)\left(1 - \frac{\epsilon}{2}\right)} \tag{27}$$

where ζ is given in Eq. 85. Now we get the following result for $\mathcal{M}_{gse_2}$:

$$\begin{aligned} \Pi_t^2 &= \frac{-ig^4 C_A T_F \, \mu^\epsilon}{2(n-1)} \int \frac{d^n k \, \pi(k^2, m^2)}{(2\pi)^n} \left\{ \frac{3n - \frac{7}{2}}{(k+q)^2} + \frac{n - 1 - \frac{1}{n}}{k^2} + q^2 \frac{3n - \frac{7}{2}}{(k+q)^2 k^2} + \left(n - \frac{3}{2}\right) \left(\frac{1}{q^2} - \frac{k^2}{q^2 (k+q)^2} + \right.\right. \\ &\left.\left. q^2 \frac{k^2 + 2kq}{(k+q)^2 k^4} \right) \right\} \end{aligned} \tag{28}$$

$$\Pi_l^2 = \frac{-ig^4 C_A T_F \, \mu^\epsilon}{2} \int \frac{d^n k \, \pi(k^2, m^2)}{(2\pi)^n} \left\{ \frac{n + \frac{1}{n} - \frac{3}{2}}{k^2} + \frac{1}{(k+q)^2} + \frac{\frac{3}{2} - n}{q^2} - \frac{q^2}{2(k+q)^2 k^2} + \left(n - \frac{3}{2}\right) \frac{k^2}{q^2 (k+q)^2} \right\} \tag{29}$$

and similarly for $\mathcal{M}_{gse_3}$:

$$\Pi_t^3 = \frac{-ig^4 C_A T_F \, \mu^\epsilon}{2(n-1)} \int \frac{d^n k}{(2\pi)^n} \pi(k^2, m^2) \left\{ \frac{6n - 2n^2 + \frac{2}{n} - 6}{k^2} \right\} \tag{30}$$

$$\Pi_l^3 = \frac{-ig^4 C_A T_F \, \mu^\epsilon}{2} \int \frac{d^n k}{(2\pi)^n} \pi(k^2, m^2) \left\{ \frac{4 - 2n - \frac{2}{n}}{k^2} \right\} \tag{31}$$

All the necessary integrals are given in appendix B. For the vertex correction graphs we arrive at the following representations:

$$\mathcal{M}_{vc_1} = \frac{ig^6 C_F C_A T_F\ \eta^\epsilon}{2(4\pi)^4 q^2}\int_0^1 dx\int_0^1 dy\int_0^1 du\int_0^1 dv\ \ x\,u\left[-\frac{B(1-u)^{\frac{\epsilon}{2}-1}\Gamma(\epsilon)}{2\alpha^{2+\frac{\epsilon}{2}}\left(\frac{-q^2}{m^2}\left(-\frac{\sigma^2}{\alpha^2}+\frac{\rho}{\alpha}\right)+\frac{1-u}{\alpha}\right)^\epsilon}\right.$$
$$\left.-\frac{(a+nb)(1-u)^{\frac{\epsilon}{2}}\Gamma(\epsilon)}{2\alpha^{3+\frac{\epsilon}{2}}\left(\frac{-q^2}{m^2}\left(-\frac{\sigma^2}{\alpha^2}+\frac{\rho}{\alpha}\right)+\frac{1-u}{\alpha}\right)^\epsilon}+\frac{c(1-u)^{\frac{\epsilon}{2}}\Gamma(1+\epsilon)}{\alpha^{3+\frac{\epsilon}{2}}\left(\frac{-q^2}{m^2}\left(-\frac{\sigma^2}{\alpha^2}+\frac{\rho}{\alpha}\right)+\frac{1-u}{\alpha}\right)^{1+\epsilon}}\right] \tag{32}$$

where σ is given by Eq. 126, ρ by Eq. 127 and α by Eq. 85. The remaining abbreviations read:

$$B \equiv -24(1-x)+8+\epsilon(12(1-x)-4) \tag{33}$$
$$a \equiv -16x(1-x)^2 \tag{34}$$
$$b \equiv 12x(1-x)^2 \tag{35}$$
$$c \equiv (8-12x)+\frac{q^2}{m^2}\left[\frac{\sigma^2}{\alpha^2}12x(1-x)^2+8(1-x)x(1-y)-12(1-x)x^2(1-y)^2+4(x^2(1-y)^2-\right.$$
$$\left.x(1-y))-2\left(12(1-y)x(1-x)^2-8(1-x)x(1-y)+4x(1-x)\right)\frac{\sigma}{\alpha}\right] \tag{36}$$

The HQET Feynman rules of Fig. 1 project all three Lorentz indices to zero for $\mathcal{M}_{vc_1}$. The completely antisymmetric nature of the three gluon vertex then implies that there is no divergence coming out of the internal fermion loop. Although Eq. 32 appears to possess a double pole, the $\frac{1}{1-u}$ " divergence" is actually finite when integrated over all Feynman parameters. We checked this directly with VEGAS [25] and it indeed gives a well converged numerical answer. As for $\mathcal{M}_{vc_2}$, we integrate out the fermion loop as before, which yields:

$$\mathcal{M}_{vc_2} = \frac{-ig^6 C_F C_A T_F}{2q^2}\int\frac{d^nk}{(4\pi)^n}\pi(k^2,m^2)\left[-\frac{k^2+2kq}{(k+q)^2k^4}+\right.$$
$$\left.\frac{1}{2(n-1)}\left(\frac{1}{(k+q)^2k^2}+\frac{1}{2}\left(\frac{k^2+2kq}{(k+q)^2k^4}+\frac{1}{q^2k^2}-\frac{1}{q^2(k+q)^2}\right)\right)\right] \tag{37}$$

All the integrals left are given in appendix B.

3.1 Infra-Red Cancellations

In this section we turn to diagrams which give integrals already present in an Abelian theory, however, which do not contribute in QED due to a cancellation that fails in the case of QCD. The reason is as follows: The color factors for the ladder diagrams are proportional to C_F^2 for the straight and $C_F^2-\frac{C_AC_F}{2}$ for the crossed ladder graph. The same structure is also present in graphs Eq. 10 and 12. In the sum of all four occurring ladder diagrams with one fermion loop plus $\mathcal{M}_{vc_3}$ and $\mathcal{M}_{olvc}$, all terms proportional to C_F^2 give a contribution that is

equal to the product of the one loop fermion graph with the Born contribution. This is an explicit example of the aforementioned exponentiation that occurs on the level of the potential. In an Abelian theory one thus has to omit these contributions.

On the other hand, in QCD, we need to calculate the crossed ladder terms and keep only the $-\frac{C_A C_F}{2}$ part of the above color factors.

From direct inspection it is furthermore obvious that these diagrams contain infra-red (IR) divergent terms which have to cancel in the potential. It has been shown in Refs. [41, 21] that the sum of $\mathcal{M}_{cl} + \mathcal{M}_{vc_3} + \mathcal{M}_{olvc}$ is IR-finite. This requirement poses a strong check on the calculation and necessitates the calculation of the IR-divergent parts of a diagram that vanishes in dimensional regularization ($\mathcal{M}_{olvc}$), i.e. when UV- and IR-divergences are not separated.

The presence of the square of the heavy quark propagator complicates the calculation of the crossed ladder diagram considerably as it makes the analytical separation of the double and single pole terms extremely difficult. We therefore found it most convenient to introduce a gluon mass λ as an IR-regulator. This allows to explicitly differentiate between UV- and IR-divergences and provides a strong numerical check on the sum of all IR-divergent contributions. In this case we get the following integral representations for the unrenormalized and IR-regulated amplitudes:

$$\mathcal{M}_{cl} = \frac{ig^6 C_F C_A T_F}{2} \int \frac{d^n k}{(4\pi)^n} \frac{\pi(k^2, m^2)(k^2 - k_0^2)}{(k_0 + i\varepsilon)^2 (k^2 - \lambda^2 + i\varepsilon)^2 ((k+q)^2 - \lambda^2 + i\varepsilon)} \tag{38}$$

$$\mathcal{M}_{vc_3} = \frac{-ig^6 C_F C_A T_F}{2q^2} \int \frac{d^n k}{(4\pi)^n} \frac{\pi(k^2, m^2)(k^2 - k_0^2)}{(k_0 + i\varepsilon)^2 (k^2 - \lambda^2 + i\varepsilon)^2} \tag{39}$$

$$\mathcal{M}_{olvc} = \frac{-ig^6 C_F C_A T_F}{2q^4} \pi(q^2, m^2) \int \frac{d^n k}{(4\pi)^n} \frac{1}{(k_0 + i\varepsilon)^2 (k^2 - \lambda^2 + i\varepsilon)} \tag{40}$$

For the contributions of graphs 38 and 39 in which the k_0^2 terms in the numerator cancel the heavy quark propagator, no gluon mass regulator in needed. The sum of these k_0-independent parts of $\mathcal{M}_{cl}$ and $\mathcal{M}_{vc_3}$ are separately IR-finite and indeed proportional to the integral 135 in appendix B. We therefore restrict ourselves to a discussion of the k_0-dependent contributions only. In these integrals the i-ε prescription is crucial in order to arrive at the correct location of poles and branch cuts the in the complex $k_0 - plane$. The presence of the fermion mass brings about a complicated integral over a general power, which in turn leads to a branch cut in the upper half of the plane. After integrating over k_0 in such a fashion one is left with an Euclidean integral over $(n-1)$-dimensions. More details and complete results are given in appendix B.1.

4 Renormalization

In Fig. 4 we list the relevant counterterms for the two loop diagrams of Fig. 2 and Fig. 3. The counterterms themselves contain non-local contributions, i.e. non-polynomial in the momentum transfer q, that have to cancel the non-local terms from the original amplitudes. The construction of the local wave function renormalization constants provides a powerful test of the correctness of the results presented both in section 3 and the appendices as they must combine successfully to arrive at the required local double and single pole terms. It might be helpful to expound on the general treatment of masses within the corresponding integrals and counterterms in the MS-renormalization scheme [4, 23]. In the counterterm approach, their contribution is restricted to finite changes through the counterterms as the wave function renormalization constants are independent of the fermion masses. In other words, all pole terms that contain masses represent non-local infinities which must cancel in the sum of graphs contributing to the overall field strength renormalization. There is therefore no difference in the formal treatment of the mass parameter in graph 7 and any other graph. This is another way of saying that the parameters of a MS-renormalized theory are not physical. Rather, they are related to measurable quatities by a perturbative series in the physical parameters.

We begin by presenting the results for the counterterms corresponding to Fig. 4. All two point counterterms correspond to the transverse parts of the gluon self energy contribution only, as these are the only relevant ones for this work. The graph $\mathcal{M}_{gse_1}$ has two counterterms, one stemming from the fermion loop divergence ($\Pi_{ct_{1f}}$) and one from the loop around the three gluon vertex ($\Pi_{ct_{1g}}$). They are given in the MS-renormalization scheme:

$$
\begin{aligned}
\Pi_{ct_{1_f}} &= \frac{-8ig^4 C_A T_F}{3(4\pi)^4\epsilon}\int_0^1 dx\Bigg[(8-6n)\,\frac{n}{2}\left(\frac{n}{2}m^2\Gamma\Big(-1+\frac{\epsilon}{2}\Big)\Big(-\frac{q^2}{m^2}x(1-x)\Big)^{1-\frac{\epsilon}{2}} - q^2x^2\Gamma\Big(\frac{\epsilon}{2}\Big)\Big(-\frac{q^2}{m^2}x(1-x)\Big)^{-\frac{\epsilon}{2}}\right) \\
&\quad -(4n-6)\left(\frac{m^2}{2}\Gamma\Big(-1+\frac{\epsilon}{2}\Big)\Big(-\frac{q^2}{m^2}x(1-x)\Big)^{1-\frac{\epsilon}{2}} - q^2x^2\Gamma\Big(\frac{\epsilon}{2}\Big)\Big(-\frac{q^2}{m^2}x(1-x)\Big)^{-\frac{\epsilon}{2}}\right) + \Big(q^2\,(-2+2n)\,x \\
&\quad +q^2\,(5n-5)\,\Gamma\Big(\frac{\epsilon}{2}\Big)\Big(-\frac{q^2}{m^2}x(1-x)\Big)^{-\frac{\epsilon}{2}}\Big)\Bigg]\,\frac{\eta^{\frac{\epsilon}{2}}}{n-1} \qquad (41) \\
\Pi_{ct_{1_g}} &= \frac{6ig^4 C_A T_F}{(4\pi)^4\epsilon}\int_0^1 dx\,\Bigg[(4n-12)\left(-\frac{n}{2}m^2\Gamma\Big(-1+\frac{\epsilon}{2}\Big)\Big(-\frac{q^2}{m^2}x(1-x)+1\Big)^{1-\frac{\epsilon}{2}} + q^2x^2\Gamma\Big(\frac{\epsilon}{2}\Big)\Big(-\frac{q^2}{m^2}x(1-x)+\right. \\
&\quad \left.1\Big)^{-\frac{\epsilon}{2}}\right) - (4n-4)(m^2+q^2x)\Gamma\Big(\frac{\epsilon}{2}\Big)\Big(-\frac{q^2}{m^2}x(1-x)+1\Big)^{-\frac{\epsilon}{2}} - 4m^2\Gamma\Big(-1+\frac{\epsilon}{2}\Big)\Big(-\frac{q^2}{m^2}x(1-x)+1\Big)^{1-\frac{\epsilon}{2}}
\end{aligned}
$$

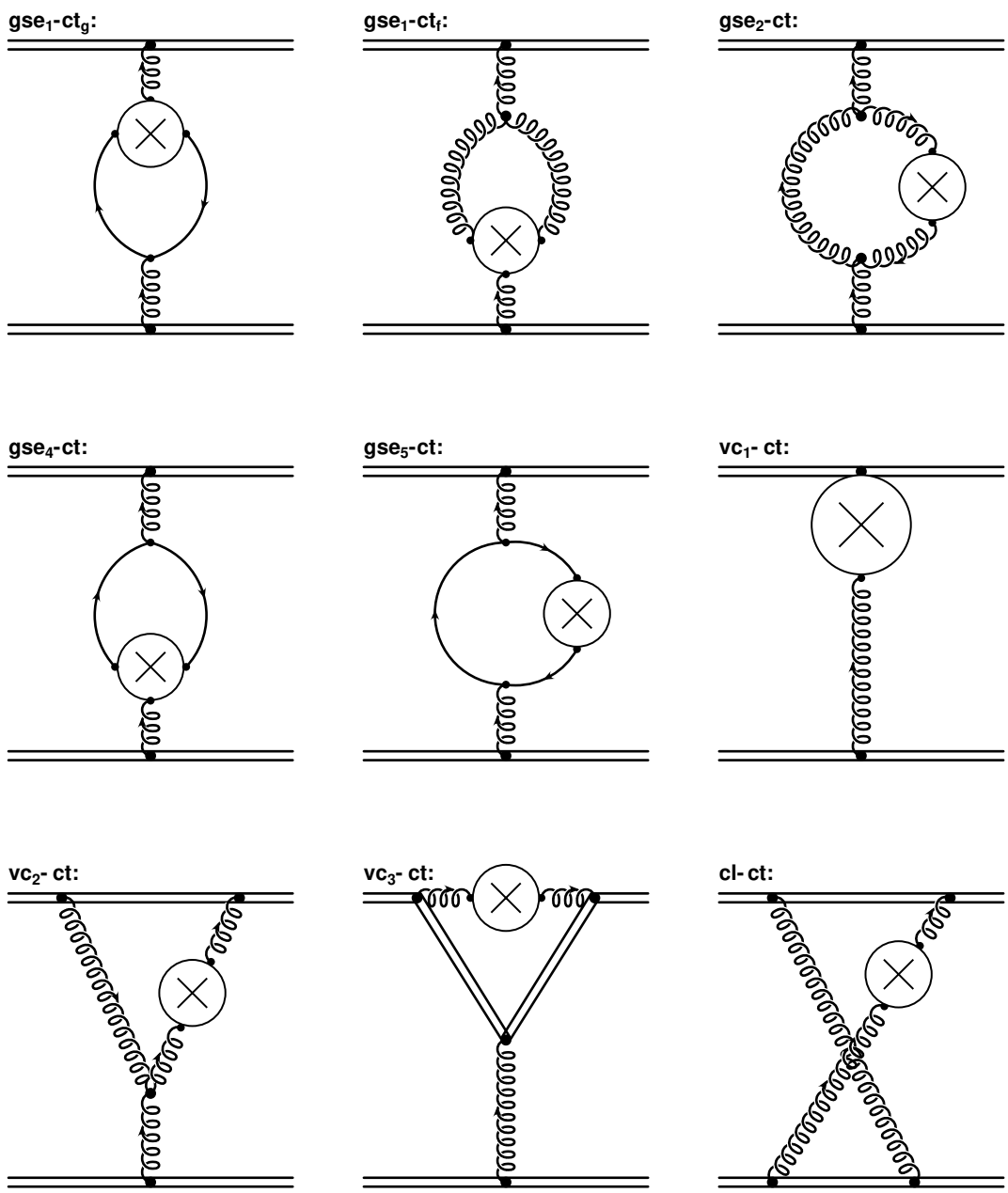

Figure 4: The two loop counterterms corresponding to the diagrams in Figs. 2 and 3. Adding these contributions to the original graphs removes all non-local functions from the occurring pole terms. The only exception are $\frac{m^2}{\epsilon}$ terms in the two point functions which only cancel in the sum of all two point diagrams as explained in the text. The fact that the tadpole diagram has no counterterm is already indicative of this cancellation.

$$-q^2x^2\Gamma\left(\frac{\epsilon}{2}\right)\left(-\frac{q^2}{m^2}x(1-x)+1\right)^{-\frac{\epsilon}{2}}\Bigg]\frac{\eta^{\frac{\epsilon}{2}}}{n-1} \tag{42}$$

For the counterterm for $\mathcal{M}_{gse_2}$ we find:

$$\Pi_{ct_2}=\frac{4ig^4C_AT_F\ q^2\zeta^{\frac{\epsilon}{2}}}{3(4\pi)^4\epsilon(n-1)}\left(\left(\frac{7}{2}-3n\right)\frac{\Gamma\left(\frac{\epsilon}{2}\right)\Gamma^2\left(1-\frac{\epsilon}{2}\right)}{\Gamma\left(2-\epsilon\right)}+\left(n-\frac{3}{2}\right)\frac{\Gamma\left(1+\frac{\epsilon}{2}\right)\Gamma\left(1-\frac{\epsilon}{2}\right)\Gamma\left(-\frac{\epsilon}{2}\right)}{\Gamma\left(1-\epsilon\right)}\right) \tag{43}$$

where η and ζ are defined in appendix B. For $\mathcal{M}_{gse_3}$ there is no counterterm as the subdivergence is independent of the mass which means that in dimensional regularization all the remaining integrals vanish.

The pole terms for the respective terms, expanded up to $\mathcal{O}\left(\epsilon^0\right)$, thus read:

$$\left[\Pi_t^1+\Pi_{ct_{1_f}}+\Pi_{ct_{1_g}}\right]_{\mathcal{O}(\epsilon^0)} = -\frac{ig^4C_AT_F\ q^2}{(4\pi)^4}\left(\frac{1}{9\epsilon^2}+\frac{163}{108\epsilon}-\frac{3m^2}{q^2\epsilon}\right) \tag{44}$$

$$\left[\Pi_t^2+\Pi_{ct_2}\right]_{\mathcal{O}(\epsilon^0)} = -\frac{ig^4C_AT_F\ q^2}{(4\pi)^4}\left(-\frac{44}{9\epsilon^2}+\frac{25}{27\epsilon}+\frac{15m^2}{q^2\epsilon}\right) \tag{45}$$

$$\left[\Pi_t^3\right]_{\mathcal{O}(\epsilon^0)} = \frac{ig^4C_AT_F\ 18m^2}{(4\pi)^4\epsilon} \tag{46}$$

These equations contain no non-local terms other than the $\frac{m^2}{\epsilon}$ terms, which then have to vanish in the sum of all contributions to the non-Abelian part of the gluon wave function renormalization constant. Because of the very involved nature of the occurring non-local terms, this is already powerful evidence of the correct evaluation of both the two loop integrals as well as the decomposition of graph $\mathcal{M}_{gse_1}$. Multiplying each graph with its respective multiplicity we find in the MS-scheme:

$$\left\{4\left[\Pi_t^1+\Pi_{ct_{1_f}}+\Pi_{ct_{1_g}}\right]+2\left[\Pi_t^2+\Pi_{ct_2}\right]+\left[\Pi_t^3\right]\right\}_{\mathcal{O}(\epsilon^0)}=\frac{ig^4C_AT_F\ q^2}{(4\pi)^4}\left(\frac{28}{3\epsilon^2}-\frac{71}{9\epsilon}\right) \tag{47}$$

This is completely local and thus demonstrates that the renormalization has been carried out properly and that the integrals given are correct. In order to further check this term we need the pole term from the "overlapping" Abelian two point diagram from Eq. 6 (which in QCD develops a color factor proportional to $(C_F-\frac{1}{2}C_A)$ in order to get the fermionic part of the overall gluon wave function renormalization constant Z_3. The counterterm for $\mathcal{M}_{gse_4}$ reads

$$\Pi_{ct_4}=-\frac{8\ i\ g^4}{\epsilon(4\pi)^2}\left(C_F-\frac{C_A}{2}\right)T_F\ q^2\ \ \pi\left(q^2,m^2\right) \tag{48}$$

and gives in agreement with [12]:

$$\left\{\left[\Pi_t^4+\Pi_{ct_4}\right]\right\}_{\mathcal{O}(\epsilon^0)}=\frac{ig^4(C_F-\frac{C_A}{2})T_F\ q^2}{(4\pi)^4}\left(\frac{16}{3\epsilon^2}-\frac{52}{9\epsilon}\right) \tag{49}$$

Adding Eqs. 47 and the C_A term of 49 gives the correct non-Abelian fermionic part of the gluon wave function renormalization constant ((times $\frac{1}{iq^2}$) see Ref. [36] for example) in the Feynman gauge:

$$Z_{3_{fermionic}}^{C_A} = \frac{g^4 C_A T_F}{(4\pi)^4}\left(\frac{20}{3\epsilon^2} - \frac{5}{\epsilon}\right) \tag{50}$$

This testifies to the overall correctness of both the decompositions used as well as all the integrals listed in the appendices!

For completeness we also give the counterterm for $\mathcal{M}_{gse_5}$, which in the MS-scheme must be treated in the same way as the graphs before. All divergent terms proportional to m^2 cancel the corresponding non-local infinities in Eq. 23:

$$\begin{aligned}\Pi_{ct_5} &= -\frac{4\ i\ g^4 C_F T_F}{\epsilon(n-1)(4\pi)^2}\Big[n\left(12m^2B_{22} + 2q^2B_{12} - 4A_2 - 12q^2m^2C_{122}\right) + (24q^2m^2 - 48m^4)C_{122} \\ &\quad -24m^2B_{22} - (4q^2 + 16m^2)B_{12} + 8A_2\Big]\end{aligned} \tag{51}$$

with

$$\left\{\left[\Pi_t^5 + \Pi_{ct_5}\right]\right\}_{\mathcal{O}(\epsilon^0)} = \frac{ig^4 C_F T_F\ q^2}{(4\pi)^4}\left(-\frac{8}{3\epsilon^2} + \frac{8}{9\epsilon}\right) \tag{52}$$

It is an important difference to the massless case that the counterterms 48 (rather its C_F part) and 51 are not related by a simple minus sign as implied by the Ward identity. There is an additional constant term $4m$ which gives new contributions. For the purely Abelian fermionic part of the gluon wave function renormalization constant in the Feynman gauge we find in agreement with Ref. [36]:

$$Z_{3_{fermionic}}^{C_F} = \frac{g^4 C_F T_F}{(4\pi)^4}\left(-\frac{4}{\epsilon}\right) \tag{53}$$

The cancellation of the higher order (double) pole is a characteristic feature in QED that holds to all orders [31].

For $\mathcal{M}_{vc_1}$ we do not need to remove non-local terms as the fermion loop is finite due to the projection of all three Lorentz indices to zero. It is easy to check this by calculating all divergent pieces after the integration of the fermion loop. All that is left is the divergence from the remaining integral which has to be subtracted in the usual MS-fashion. This is indicated in Fig. 4. The explicit pole term is given by:

$$[\mathcal{M}_{vc1}]_{\mathcal{O}(\epsilon^0)} = \frac{ig^6 C_F C_A T_F}{(4\pi)^4 q^2}\left(-\frac{1}{\epsilon}\right) \tag{54}$$

in agreement with the massless case [20]. In the case of $\mathcal{M}_{vc_2}$ we do have non-local terms, and the counterterm reads:

$$\begin{aligned}\mathcal{M}_{vc2_{ct}} &= \frac{4ig^6 C_F C_A T_F\, \eta^{\frac{\epsilon}{2}}}{3(4\pi)^4 q^2 \epsilon} \int_0^1 dv \left(-\frac{nv\Gamma\left(\frac{\epsilon}{2}\right)}{2(\frac{-q^2}{m^2}v(1-v))^{\frac{\epsilon}{2}}} + \frac{(1+v)\Gamma\left(1+\frac{\epsilon}{2}\right)}{(\frac{-q^2}{m^2}v(1-v))^{\frac{\epsilon}{2}}} + \right. \\ &\left. \frac{\Gamma\left(\frac{\epsilon}{2}\right)}{2(n-1)(\frac{-q^2}{m^2}v(1-v))^{\frac{\epsilon}{2}}} + \frac{nv\Gamma\left(\frac{\epsilon}{2}\right)}{8(n-1)(\frac{-q^2}{m^2}v(1-v))^{\frac{\epsilon}{2}}} - \frac{(1+v)\Gamma\left(1+\frac{\epsilon}{2}\right)}{4(n-1)(\frac{-q^2}{m^2}v(1-v))^{\frac{\epsilon}{2}}} \right) \end{aligned} \tag{55}$$

Adding Eq. 55 with the appropriate normalization and color factors to the result given in 37 does indeed give completely local double and single pole terms as required in dimensional regularization after the subdivergences are subtracted:

$$[\mathcal{M}_{vc_2} + \mathcal{M}_{vc2_{ct}}]_{\mathcal{O}(\epsilon^0)} = \frac{ig^6 C_F C_A T_F}{(4\pi)^4 q^2} \left(\frac{1}{\epsilon^2} - \frac{5}{12\epsilon} \right) \tag{56}$$

It demonstrates that indeed all non-local divergences are canceled and agrees furthermore with the pole terms obtained in the massless analysis [20]! It should be noted that all the integrals needed were already used in the $\mathcal{M}_{gse_2}$ calculation for which such a strong internal consistency check was performed just above. All the required expansions above were carried out with the help of MAPLE in face of the complexity involved. As mentioned before, also the translation into FORTRAN was handled by MAPLE as to reduce possible accidental errors. .

4.1 Counterterms with Gluon Mass

At this point we need the counterterms of the IR-divergent contributions, $\mathcal{M}_{cl}$, $\mathcal{M}_{vc_3}$ and $\mathcal{M}_{olvc}$. As indicated above and expressed in Eqs. 38, 39 and 40, these were regulated by introducing a gluon mass regulator. The remaining UV-divergences are treated as above in the context of dimensional regularization. We therefore have to calculate all counterterm contributions that occur for gluon propagators with a gluon mass. Without such a dimensionful quantity, only the crossed ladder diagram would yield a counterterm in dimensional regularization. We again use the gluon mass only for k_0-dependent terms as explained in section 3.1. This is indicated below.

The results are obtained in a similar way as for the corresponding amplitudes, first integrating over the heavy quark propagator in the complex k_0-plane with a subsequential $(n-1)$-dimensional Euclidean integral remaining. The results are obtained straightforwardly as there are only pole terms and no branch cuts in the counterterm contributions. We find for the gluon mass regulated terms:

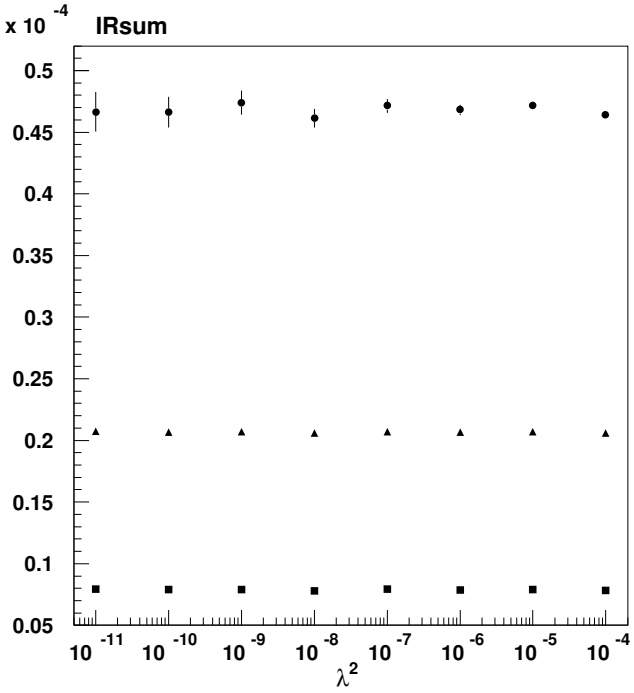

Figure 5: The sum of the λ^2-dependent amplitudes and counterterms $\mathcal{M}_{cl}^{k_0} + \mathcal{M}_{vc_3}^{k_0} + \mathcal{M}_{olvc} + \mathcal{M}_{cl_{ct}}^{k_0} + \mathcal{M}_{vc_{3\,ct}}^{k_0}$. Circles correspond to a choice of $q^2 = -10GeV^2$ and $m = m_c$, triangles to $q^2 = -100GeV^2$ and $m = m_c$ while the lower curve (squares) has $q^2 = -100GeV^2$ and $m = m_b$. The overall normalization neglects color factors and the coupling strength. All data are obtained by using 10^6 evaluations per iteration with VEGAS and 100 iterations. The statistical error is indicated and smaller than the symbols where invisible. The sum for each of the displayed sets of parameters is clearly independent of the IR-gluon mass regulator λ as expected.

$$\mathcal{M}_{cl_{ct}}^{k_0} = \frac{4ig^6 C_F C_A T_F\ \eta^{\frac{\epsilon}{2}} \Gamma\left(1+\frac{\epsilon}{2}\right)}{\epsilon(4\pi)^{\frac{7}{2}}\Gamma\left(\frac{5}{2}\right) m^2} \int_0^1 dv \frac{1}{(\frac{-q^2}{m^2}v(1-v) + \frac{\lambda^2}{m^2})^{1+\frac{\epsilon}{2}}} \tag{57}$$

$$\mathcal{M}_{vc_{3\,ct}}^{k_0} = -\frac{8ig^6 C_F C_A T_F\ \eta^{\frac{\epsilon}{2}} \Gamma\left(\frac{\epsilon}{2}\right)}{3\epsilon q^2 (4\pi)^{\frac{7}{2}}\Gamma\left(\frac{3}{2}\right)\left(\frac{\lambda^2}{m^2}\right)^{\frac{\epsilon}{2}}} \tag{58}$$

For completeness we also list the remaining counterterm stemming from the k_0-independent part of $\mathcal{M}_{cl}$:

$$\mathcal{M}_{cl_{ct}}^{k} = \frac{16ig^6 C_F C_A T_F\ 4^{\frac{\epsilon}{2}} \eta^{\frac{\epsilon}{2}} \Gamma\left(1+\frac{\epsilon}{2}\right)\Gamma\left(-\frac{\epsilon}{2}\right)}{3\epsilon m^2 (4\pi)^{\frac{7}{2}}\Gamma\left(\frac{1}{2}-\frac{\epsilon}{2}\right)\left(\frac{-q^2}{m^2}\right)^{1+\frac{\epsilon}{2}}} \tag{59}$$

The gluon mass terms that occur in the expansion of the original as well as the counterterms above in powers of ϵ in the pole terms of dimensional regularization represent now non-local divergences which have to cancel

in the same way as terms containing m^2 or non-polynomial functions of q^2. The remaining IR-divergent pole terms are contained in the form of logarithmic divergences in λ. Fig. 5 demonstrates that in the sum of the IR-divergent amplitudes plus their corresponding counterterms no λ-dependence is left within the statistical errors. For convenience, three sets of values for q^2 and m^2 are displayed while the renormalization scale μ remains fixed. We have checked that it also holds for a variety of other choices of parameters. Some need fewer evaluations to converge while others need up to 10^7 per iteration.

It is perhaps interesting to note that the crossed ladder diagram, naively only singly IR-divergent, actually possesses a quadratic divergence in $log(\lambda)$ which cancels the (also unexpected) quadratic divergence in the Abelian vertex correction term. The remaining UV-divergent pole terms in the MS-scheme are found to be:

$$\left[\mathcal{M}_{cl}^{k_0} + \mathcal{M}_{cl_{ct}}^{k_0}\right]_{\mathcal{O}(\epsilon^0)} = 0 \tag{60}$$

$$\left[\mathcal{M}_{vc_3}^{k_0} + \mathcal{M}_{vc_{3_{ct}}}^{k_0}\right]_{\mathcal{O}(\epsilon^0)} = \frac{ig^6 C_F C_A T_F}{(4\pi)^4 q^2}\left(-\frac{16}{3\epsilon^2} + \frac{80}{9\epsilon}\right) \tag{61}$$

$$\left[\mathcal{M}_{cl}^{k} + \mathcal{M}_{vc_3}^{k} + \mathcal{M}_{cl_{ct}}^{k}\right]_{\mathcal{O}(\epsilon^0)} = \frac{ig^6 C_F C_A T_F}{(4\pi)^4 q^2}\left(-\frac{16}{3\epsilon^2} + \frac{16}{9\epsilon}\right) \tag{62}$$

which states that the counterterm in case of $\mathcal{M}_{cl}^{k_0}$ completely remove all pole terms in ϵ. It is also clear that all non-local terms are removed by the appropriate counterterms as was expected. In order to compare this with the results obtained in the massless case one would need to differentiate between ϵ_{UV} and ϵ_{IR}.

5 Numerical Results

At this point we have calculated all diagrams that contribute to the massive fermionic corrections to the heavy quark potential that were previously unknown. In the previous section we demonstrated that the counterterms successfully remove all non-local divergences and that the MS-subtraction terms coincide with the massless limit. The complexity of the explicit results given in the appendices raises some questions about how stable a numerical integration over up to four Feynman parameters is with VEGAS as well as about the correctness of the finite terms of these expressions. An ideal test is provided by the results obtained in Ref. [21] for the massless limit.

Fig. 6 contains the results of the IR-finite two loop amplitudes from Figs. 2 and 3 in section 2. The tadpole diagram vanishes trivially in that limit so that only the six graphs shown remain. The sames choices for q^2

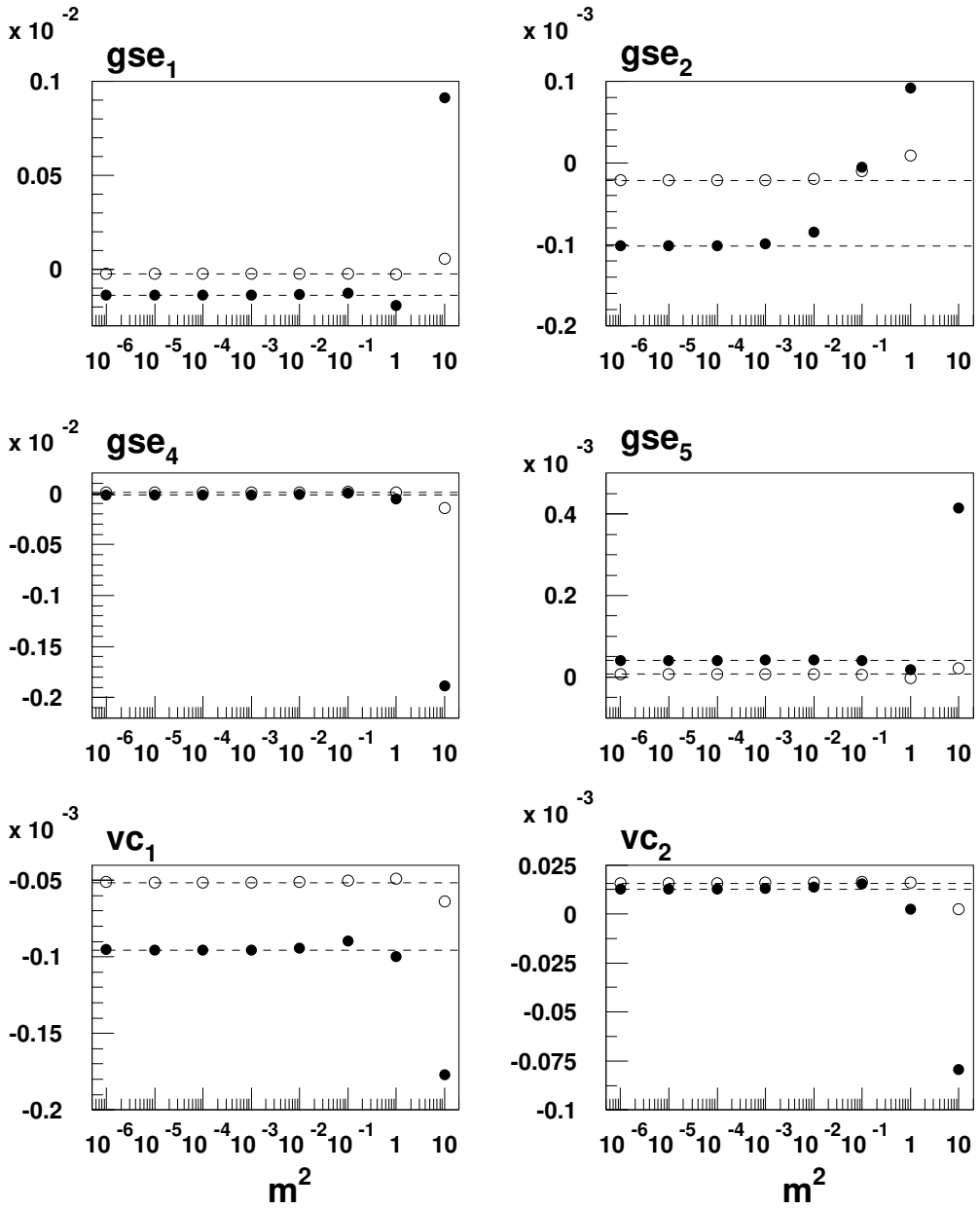

Figure 6: A comparison of the six amplitudes $\mathcal{M}_{gse_1}$, $\mathcal{M}_{gse_2}$, $\mathcal{M}_{gse_4}$, $\mathcal{M}_{gse_5}$, $\mathcal{M}_{vc_1}$ and $\mathcal{M}_{vc_2}$ with the massless limit (dashed lines) [20] in the MS-scheme. Solid circles correspond to a choice of $q^2 = -1.5\ GeV^2$, open ones to $q^2 = -4.5\ GeV^2$. $\mu = 0.31\ GeV$ in each case. Each graph begins to deviate from the massless limit only when m^2 is of the same order as $-q^2$ as expected. These results were obtained after 10^6 evaluations per iteration and after 50 iterations. The statistical error is smaller than the size of the symbols and the normalization neglects color factors and the coupling strength.

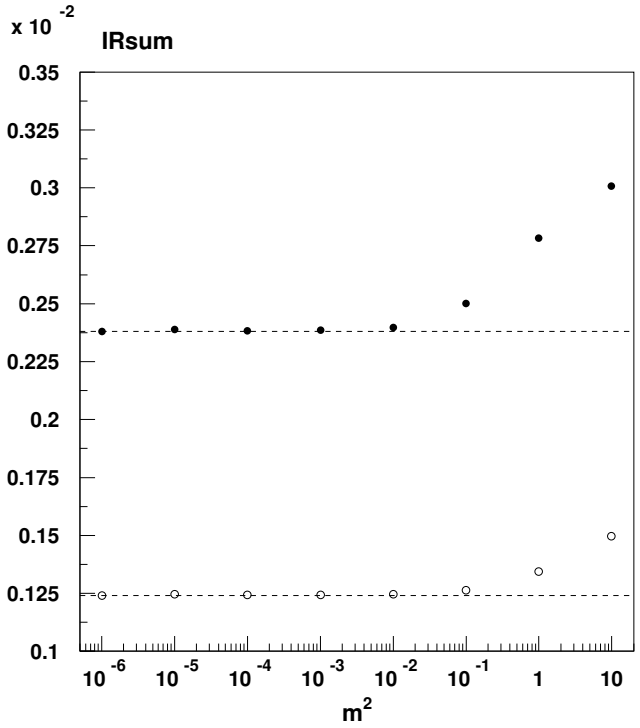

Figure 7: A comparison of the sum of amplitudes $\mathcal{M}_{cl}+\mathcal{M}_{vc_3}+\mathcal{M}_{olvc}$ plus their MS-counterterms with the massless limit (dashed lines) [20]. Solid circles correspond to a choice of $q^2 = -1.5\ GeV^2$, open ones to $q^2 = -4.5\ GeV^2$. $\mu = 0.031\ GeV$ and $\lambda^2 = 10^{-8}$ in each case. The sum begins to deviate from the massless limit only when m^2 is of the same order as $-q^2$ as was the case for the other graphs. These results were obtained after 10^6 evaluations per iteration and after 100 iterations. The statistical error is smaller than the size of the symbols and the normalization neglects color factors and the coupling strength.

and the renormalization scale μ were made in all six plots. Since the results of Ref. [21] were calculated in the $\overline{MS}$-renormalization scheme, we use

$$\mu_{MS} = \sqrt{\frac{e^\gamma}{4\pi}}\mu_{\overline{MS}} \tag{63}$$

It is clear from these results that deviations from the massless limit only occur when $m^2 \approx -q^2$ or greater. This was of course expected and the motivation for this calculation. A similar dependence is observed for the sum of the three IR-divergent amplitudes from Fig. 2 in section 2. Here it is impossible to compare on an amplitude by amplitude level since a different IR-regulator was used. Only the sum of infra-red finite contributions can be compared at the two loop level. We checked explicitly that by replacing $log(\lambda)$ with $\frac{1}{\epsilon}$, only the double pole terms can be seen to be identical.

The single pole terms differ and so do the finite contributions for each amplitude. In the sum, however, the IR-divergent pieces cancel (as demonstrated in Fig. 5), and here we can find a meaningful comparison. Fig. 7 demonstrates that the correct massless limit is indeed recovered. The numerical accuracy in terms of the statistical error from the VEGAS Monte Carlo integration is actually included in the figures. It is better than 1% though, and thus not visible on the scale of the plots. The gluon mass regulated graphs were evaluated over twice as many iterations (100) compared to the graphs from Fig. 6 as the required cancellations are numerically more unstable. In both cases the number of evaluations per iteration is 10^6.

Fig. 8 displays the sums of all non-Abelian as well as the sum of all Abelian fermionic contributions to the heavy quark potential. In addition we included the one loop corrections (bottom) in the MS-scheme (omitting coupling constants) as given in Eq. 26. The simple logarithmic behavior of the massless one loop result is clearly visible and asymptotically approached by the massive curves. The sign of the one loop correction is opposite to the two loop Abelian result, reflecting the fact that effectively for large momenta $\beta_0^{QED} \longrightarrow \left(\beta_0^{QED}\right)^2$ (in the massless case, with $\beta_0^{QED} = -\frac{2}{3}$). The relative size of the mass effects are comparable for the one and two loop corrections.

The massless two loop results can be seen to possess the expected double logarithmic contributions. The massive two loop results show an almost completely opposite behavior for low values of $\frac{m^2}{-q^2}$. At the flavor thresholds, though, both contributions increase the value obtained from the massless case by the same (relative) order of magnitude. The overall corrections are much larger in absolute terms for the non-Abelian case, partially due to an extra factor of C_A, while in relative terms the Abelian corrections are bigger. In the high energy regime both graphs show that the massless limit is approached asymptotically.

The complete massive fermionic two loop contributions to the heavy quark potential are presented in Fig. 9. It can be seen that the overall curve is dominated by the non-Abelian threshold behavior (partially due to the extra factor of C_A). The "m_c-graph" (triangles) matches the massless case for lower values of $-q^2$ as $m_c^2 \ll m_b^2$. At the respective thresholds we find roughly a 33 % deviation relative to the massless case. This could be very significant for applications where quark masses are expected to play an important part. Furthermore, the physically defined effective charge $\alpha_V(\mathbf{q^2}, m^2)$ incorporates quark masses naturally at the flavor thresholds and is also analytic. Thus, there is no problem of evolving the strong coupling constant through these thresholds and one never needs to impose matching conditions. At high values of $\mathbf{q^2}$ the theory becomes massless and reproduces the leading logarithmic terms obtained by the β-function analysis as these coefficients are scheme independent through two

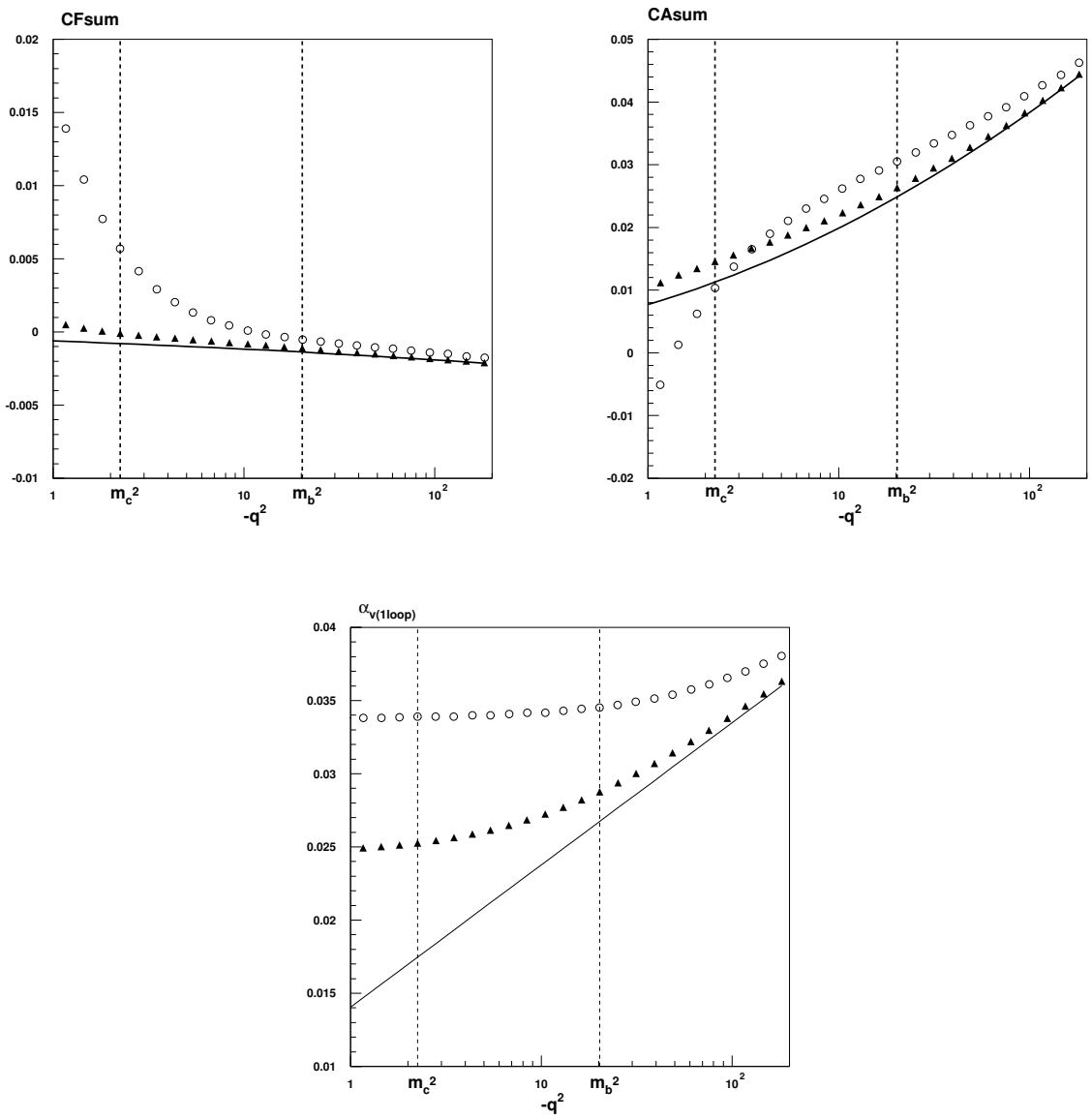

Figure 8: The mass dependence of α_V at one (bottom) and two loops. The two loop case is displayed in terms of all Abelian terms (left) and for all non-Abelian terms (proportional to C_A). Triangles denote $m^2 = m_c^2 = (1.5GeV)^2$ and open circles $m^2 = m_b^2 = (4.5GeV)^2$. The massless case is also included (line). All curves have the same value of the renormalization scale $\mu = 0.031$. It is clearly visible that the flavor threshold behavior is quite similar in the three figures with an opposite tendency for low values of $-q^2$ in the two loop case though. The one loop corrections have an opposite sign relative to the Abelian two loop corrections. The coupling constants are omitted. All cases approach the massless limit when $\frac{m^2}{-q^2} \ll 1$.

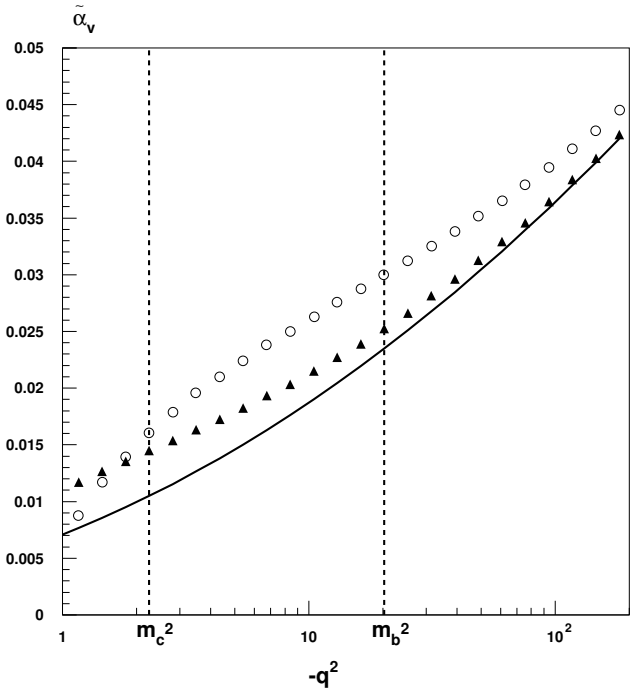

Figure 9: The complete two loop mass dependence of $\tilde{\alpha_V} \equiv \frac{\alpha_V^{f\,2\,loop}}{g^6}$ for $m^2 = m_c^2 = (1.5GeV)^2$ (triangles) and $m^2 = m_b^2 = (4.5GeV)^2$ (open circles). The massless case is also included (line). In all three curves we use $\mu = 0.031$. The deviation from the massless case at the flavor thresholds is of order of 33% and is dominated by the new non-Abelian contributions

loops in a massless theory.

The above analysis can also be helpful for the incorporation of massive fermions in lattice analyses as the heavy quark potential is defined by the gauge invariant vacuum expectation value of the Wilson loop in Eq. 1. For a direct application of the presented results, a recently proposed way of incorporating quark flavor thresholds by relating the "natural" heavy quark potential m_q-dependence to an effective continuous and smooth function $n_F(-q^2, m^2)$ [30] seems to be a promising candidate.

6 Conclusions

We have calculated all the necessary integrals for the non-Abelian massive fermionic corrections to the heavy quark potential through two loops. They describe the analytic flavor thresholds of the physical coupling $\alpha_V(\mathbf{q^2}, m^2)$. The new results were obtained by using a mixed analytical, computer-algebraic as well as numerical approach and strong consistency checks were performed by observing that all non-local divergences cancel by adding the

appropriate counterterms. In case of the complicated two point diagrams it is found that the weighted sum of all diagrams gives the correct local gluon wave function renormalization constant. The renormalization constants were given explicitly.

It was also checked that no spurious infra-red divergences were introduced by the implemented reduction scheme as they are present in the intermediate steps of the calculation. For the explicitly IR-divergent diagrams we proved that no physical results depend on the introduction of the gluon mass regulator λ. This is a consequence of the color singlet state of the external heavy quark sources.

All physically interesting and gauge invariant finite parts were integrated with VEGAS [25] and found to agree perfectly with the massless results of Ref. [22] in that limit which actually checks this part of the analysis in [21]. The difference to the massless case around the charm and bottom flavor thresholds was found to be roughly 33%. The size of this effect can have important consequences for processes in which one cannot neglect these masses as well as for the evolution of the strong coupling constant through analytic flavor thresholds.

A Decomposition of Two Loop Tensor Integrals

For the gluon self energy graphs $\mathcal{M}_{gse_1}$, $\mathcal{M}_{gse_4}$ and $\mathcal{M}_{gse_5}$ we chose to not do the fermion loop integral first, as we did for all vacuum polarization insertions, but to decompose the occurring tensor integrals into a linear combination of scalar two loop integrals. The scalar integrals entering in the expression given in Eq. 18 (or 20) will be treated in detail in the next section together with all other integrals needed in this work.

We work in n space-time dimensions, $n = 4 - \epsilon$, and for the two loop integrals we use the following notation:

$$[1] \equiv (l+q)^2 - m^2, [2] \equiv l^2 - m^2, [3] \equiv (l-k)^2 - m^2, [4] \equiv (k+q)^2, [5] \equiv k^2 \tag{64}$$

l denotes the loop momentum of the massive fermion loop and k the remaining loop momentum. A prime like $[2'] \equiv l^2$ denotes the massless propagator with the same momentum as the unprimed. While there are different possible technical approaches to our desired decomposition, such as the one recently suggested in Ref. [24], the general method we use follows that of Ref. [10]. We also denote integrals with squares of "denominator" terms in the numerator "Y"- integrals and pure two loop scalar integrals by "T".

In the following we use various symmetries between Y- as well as between T-integrals. For instance

$$Y^2_{1345} = Y^1_{2345} \quad , \quad T_{134} = T_{235} \tag{65}$$

For two loop scalar integrals that are actually a product of scalar one loop integrals we use the respective one loop notation of Ref. [11]. All of the decompositions were programmed in FORM [13] and lead to the following

relations for $\mathcal{M}_{gse_1}$:

$$
\begin{aligned}
Y^{11}_{2345} &\equiv \int \frac{d^nk}{(2\pi)^n}\int \frac{d^nl}{(2\pi)^n}\frac{\mu^{2\epsilon}((l+q)^2-m^2)^2}{(l^2-m^2)((l-k)^2-m^2)(k+q)^2k^2} \\
&= q^2\left(T_{235}-T_{135}\right)+\frac{1}{n-1}\left[\frac{n}{6}\left(-m^4T_{12'35}+m^2T_{135}+m^2A_2B_{12'}-m^2T_{2'35}-A_2^2\right)-m^2T_{135}\right. \\
&\quad +m^2T_{235}+\frac{n}{4}q^4T_{2345}+\frac{n}{2}q^4A_2C_{455}-m^2q^4T_{23455}-q^4A_2C_{455}+\frac{n}{6}m^2q^2T_{12'35}+\frac{7n}{12}q^2T_{135} \\
&\quad \left.-\frac{n}{4}q^2T_{135}+nq^2A_2B_{45}-\frac{n}{6}q^2A_2B_{12'}+2m^2q^2T_{2345}+m^2q^2T_{2355}-q^2T_{135}\right] \qquad (66)
\end{aligned}
$$

$$
\begin{aligned}
Y^{1}_{2345} &\equiv \int \frac{d^nk}{(2\pi)^n}\int \frac{d^nl}{(2\pi)^n}\frac{\mu^{2\epsilon}((l+q)^2-m^2)}{(l^2-m^2)((l-k)^2-m^2)(k+q)^2k^2} \\
&= A_2B_{45}+\frac{1}{2}\left(T_{235}-T_{135}+q^2T_{2345}\right) \qquad (67) \\
Y^{4}_{1235} &\equiv \int \frac{d^nk}{(2\pi)^n}\int \frac{d^nl}{(2\pi)^n}\frac{\mu^{2\epsilon}(k+q)^2}{((l+q)^2-m^2)(l^2-m^2)((l-k)^2-m^2)k^2} \\
&= A_2B_{12}+q^2T_{1235}+\frac{1}{2}\left(T_{2'35}+A_2B_{22'}-A_2B_{12'}-T_{135}-q^2A_2C_{122'}+(m^2-q^2)T_{12'35}\right) \qquad (68) \\
Y^{3}_{1245} &\equiv \int \frac{d^nk}{(2\pi)^n}\int \frac{d^nl}{(2\pi)^n}\frac{\mu^{2\epsilon}((l-k)^2-m^2)}{((l+q)^2-m^2)(l^2-m^2)(k+q)^2k^2} = A_2B_{45}-\frac{q^2}{2}B_{12}B_{45} \qquad (69) \\
Y^{1}_{234} &\equiv \int \frac{d^nk}{(2\pi)^n}\int \frac{d^nl}{(2\pi)^n}\frac{\mu^{2\epsilon}((l+q)^2-m^2)}{(l^2-m^2)((l-k)^2-m^2)(k+q)^2} \\
&= \frac{1}{3}\left[A_2^2+m^2\left(T_{2'35}-A_2B_{12'}-T_{135}+m^2T_{12'35}\right)+q^2\left(T_{135}+A_2B_{12'}-m^2T_{12'35}\right)\right] \qquad (70) \\
Y^{4}_{135} &\equiv \int \frac{d^nk}{(2\pi)^n}\int \frac{d^nl}{(2\pi)^n}\frac{\mu^{2\epsilon}(k+q)^2}{((l+q)^2-m^2)((l-k)^2-m^2)k^2} \\
&= \frac{1}{3}\left(A_2^2+q^2T_{135}\right)-\frac{2}{3}\left[m^2\left(T_{2'35}-A_2B_{12'}-T_{135}+m^2T_{12'35}\right)+q^2\left(A_2B_{12'}-m^2T_{12'35}\right)\right] \qquad (71) \\
Y^{1}_{235} &\equiv \int \frac{d^nk}{(2\pi)^n}\int \frac{d^nl}{(2\pi)^n}\frac{\mu^{2\epsilon}((l+q)^2-m^2)}{(l^2-m^2)((l-k)^2-m^2)k^2} = q^2T_{235} \qquad (72) \\
Y^{1}_{245} &\equiv \int \frac{d^nk}{(2\pi)^n}\int \frac{d^nl}{(2\pi)^n}\frac{\mu^{2\epsilon}((l+q)^2-m^2)}{(l^2-m^2)(k+q)^2k^2} = q^2A_2B_{45} \qquad (73)
\end{aligned}
$$

For the remaining two diagrams, $\mathcal{M}_{gse_4}$ and $\mathcal{M}_{gse_5}$, we have slightly different denominators as is evident from Eqs. 6 and 7. It is possible, though, to relate these to the conventions given in 64 with the exception of the finite scalar integral T^A_{12345} which is given in Eq. 128. "A" denotes the fact that the topology of these diagrams is Abelian. Below we list the Y-functions we need for the required decomposition with terms on the l.h.s. having the denominators of the original integrals and given in terms of functions on the r.h.s. which are using the conventions of Eq. 64:

$$
\begin{aligned}
{}^{A}Y^{1}_{2345} &= A_2 B_{12} + T_{235} - T_{135} + q^2 T_{1235} - Y^{4}_{1235} && (74)\\
{}^{A}Y^{3}_{1245} &= 2A_2 B_{12} + (2m^2 - \frac{q^2}{2}) B^2_{12} && (75)\\
{}^{A}Y^{4}_{2335} &= T_{235} + q^2 T_{2235} && (76)\\
{}^{A}Y^{2}_{135} &= {}^{A}Y^{5}_{234} = {}^{A}Y^{4}_{135} = {}^{A}Y^{1}_{234} = Y^{1}_{234} && (77)\\
{}^{A}Y^{4}_{235} &= q^2 T_{235} && (78)\\
{}^{A}Y^{1}_{235} &= q^2 T_{235} && (79)\\
{}^{A}Y^{4}_{255} &= A^2_2 + q^2 A_2 B_{22} && (80)
\end{aligned}
$$

B Two-Loop Integrals

In this appendix we give the explicit results for all the integrals needed in the calculation of the two loop fermionic corrections to the heavy quark potential. These include all the scalar two loop integrals occurring in the decomposition of the gluon self energy graph $\mathcal{M}_{gse_1}$ in section 3 as well as the remaining tensor integrals needed for the remaining contributions. Since the potential between two infinitely heavy color test charges represents a physical quantity, all integrals presented are real due to the spacelike value of the physical momentum transfer $q^2 < 0$. For this reason we found it convenient to adopt both analytical as well as numerical methods for the implementation into FORTRAN. Wherever possible we proceed with the integration of the remaining Feynman parameter integrals and where this becomes too involved, we integrate the remainder with the Monte Carlo integrator VEGAS, [25].

The notation is as follows:

The following Feynman parameter identities [26] are very useful and were employed in all integrals in this work:

$$
\begin{aligned}
\frac{1}{a_1 ... a_m} &= \Gamma(m) \int_0^1 du_1 ... \int_0^1 du_{m-1} \frac{u_1^{m-2} u_2^{m-3} ... \; u_{m-2}}{(a_1 u_1 ... u_{m-1} + a_2 u_1 ... u_{m-2}(1-u_{m-1}) + ... + a_m(1-u_1))^m} && (81)\\
\frac{1}{a^\alpha b^\beta} &= \frac{\Gamma(\alpha+\beta)}{\Gamma(\alpha)\Gamma(\beta)} \int_0^1 du \frac{u^{\alpha-1}(1-u)^{\beta-1}}{(au + b(1-u))^{\alpha+\beta}} && (82)\\
\frac{1}{a^\alpha b^\beta c^\gamma} &= \frac{\Gamma(\alpha+\beta+\gamma)}{\Gamma(\alpha)\Gamma(\beta)\Gamma(\gamma)} \int_0^1 du \; u \int_0^1 dv \frac{(uv)^{\alpha-1}(u(1-v))^{\beta-1}(1-u)^{\gamma-1}}{(auv + bu(1-v) + c(1-u))^{\alpha+\beta+\gamma}} && (83)\\
\frac{1}{a^\alpha b^\beta c^\gamma d^\delta} &= \frac{\Gamma(\alpha+\beta+\gamma+\delta)}{\Gamma(\alpha)\Gamma(\beta)\Gamma(\gamma)\Gamma(\delta)} \int_0^1 du \; u^2 \int_0^1 dv \; v \int_0^1 dw \frac{(uvw)^{\alpha-1}(uv(1-w))^{\beta-1}(u(1-v))^{\gamma-1}(1-u)^{\delta-1}}{(auvw + buv(1-w) + cu(1-v) + d(1-u))^{\alpha+\beta+\gamma+\delta}} && (84)
\end{aligned}
$$

We use the following abbreviations in addition:

$$
\eta \equiv \frac{4\pi\mu^2}{m^2}, \quad \zeta \equiv \frac{4\pi\mu^2}{-q^2}, \quad \alpha \equiv u + (1-u)x(1-x), \quad \widetilde{\alpha} \equiv u + (1-u)(1-x) \qquad (85)
$$

$$\Delta \equiv \frac{q^2}{m^2}\left(\frac{u^2(1-v)^2}{\alpha^2}-\frac{u(1-v)}{\alpha}\right)+\frac{1-u}{\alpha} \tag{86}$$

$$\widetilde{\Delta} \equiv \frac{q^2}{m^2}\left(\frac{u^2(1-v)^2}{\widetilde{\alpha}^2}-\frac{u(1-v)}{\widetilde{\alpha}}\right)+\frac{1}{\widetilde{\alpha}} \tag{87}$$

$$\widetilde{\Delta'} \equiv \frac{q^2}{m^2}\left(\frac{u^2(1-v)^2}{\widetilde{\alpha}^2}-\frac{u(1-v)}{\widetilde{\alpha}}\right)+\frac{1-uv}{\widetilde{\alpha}} \tag{88}$$

where μ is the dimensional-regularization mass parameter [23]. All results are given in terms of their dependence on ϵ and would have to be expanded with the factors given in the explicit results of section 3 up to $\mathcal{O}(\epsilon)$. The results in this paper were obtained by employing MAPLE to do the required expansion and are too cumbersome for explicit presentation.

We start with results of the following simple scalar one and two loop functions:

$$A_2 \equiv \int \frac{d^n l}{(2\pi)^n}\frac{\mu^\epsilon}{(l^2-m^2)} = -\frac{i\,m^2\eta^{\frac{\epsilon}{2}}\Gamma\left(-1+\frac{\epsilon}{2}\right)}{16\pi^2} \tag{89}$$

$$B_{22} \equiv \int \frac{d^n l}{(2\pi)^n}\frac{\mu^\epsilon}{(l^2-m^2)^2} = \frac{i\,\eta^{\frac{\epsilon}{2}}\Gamma\left(\frac{\epsilon}{2}\right)}{16\pi^2} \tag{90}$$

$$B_{22'} \equiv \int \frac{d^n l}{(2\pi)^n}\frac{\mu^\epsilon}{(l^2-m^2)l^2} = \frac{i\,\eta^{\frac{\epsilon}{2}}\Gamma\left(\frac{\epsilon}{2}\right)}{16\pi^2\left(1-\frac{\epsilon}{2}\right)} \tag{91}$$

$$B_{12'} \equiv \int \frac{d^n l}{(2\pi)^n}\frac{\mu^\epsilon}{((l+q)^2-m^2)l^2} = \int_0^1 dx \frac{i\eta^{\frac{\epsilon}{2}}\Gamma\left(\frac{\epsilon}{2}\right)}{(4\pi)^2(\frac{-q^2}{m^2}x(1-x)+x)^{\frac{\epsilon}{2}}} \tag{92}$$

$$B_{12} \equiv \int \frac{d^n l}{(2\pi)^n}\frac{\mu^\epsilon}{((l+q)^2-m^2)(l^2-m^2)} = \int_0^1 dx \frac{i\eta^{\frac{\epsilon}{2}}\Gamma\left(\frac{\epsilon}{2}\right)}{(4\pi)^2(\frac{-q^2}{m^2}x(1-x)+1)^{\frac{\epsilon}{2}}} \tag{93}$$

$$B_{45} \equiv \int \frac{d^n k}{(2\pi)^n}\frac{\mu^\epsilon}{(k+q)^2k^2} = \int_0^1 dx \frac{i\eta^{\frac{\epsilon}{2}}\Gamma\left(\frac{\epsilon}{2}\right)}{(4\pi)^2(\frac{-q^2}{m^2}x(1-x))^{\frac{\epsilon}{2}}} = \frac{i\zeta^{\frac{\epsilon}{2}}\Gamma\left(\frac{\epsilon}{2}\right)\Gamma^2\left(1-\frac{\epsilon}{2}\right)}{(4\pi)^2\Gamma\left(2-\epsilon\right)} \tag{94}$$

$$C_{455} \equiv \int \frac{d^n k}{(2\pi)^n}\frac{\mu^\epsilon}{(k+q)^2k^4} = \frac{i\zeta^{\frac{\epsilon}{2}}\Gamma\left(-\frac{\epsilon}{2}\right)\Gamma\left(1-\frac{\epsilon}{2}\right)\Gamma\left(1+\frac{\epsilon}{2}\right)}{q^2(4\pi)^2\Gamma\left(1-\epsilon\right)} \tag{95}$$

$$C_{122} \equiv \int \frac{d^n l}{(2\pi)^n}\frac{\mu^\epsilon}{((l+q)^2-m^2)(l^2-m^2)^2} = -\int_0^1 dx \frac{i\,x\eta^{\frac{\epsilon}{2}}\Gamma\left(1+\frac{\epsilon}{2}\right)}{(4\pi)^2m^2(\frac{-q^2}{m^2}x(1-x)+1)^{1+\frac{\epsilon}{2}}} \tag{96}$$

$$C_{122'} \equiv \int \frac{d^n l}{(2\pi)^n}\frac{\mu^\epsilon}{((l+q)^2-m^2)(l^2-m^2)l^2} = -\int_0^1 dx\int_0^1 dy \frac{i\eta^{\frac{\epsilon}{2}}\Gamma\left(1+\frac{\epsilon}{2}\right)x^{-\frac{\epsilon}{2}}}{(4\pi)^2m^2(\frac{q^2}{m^2}(x(1-y)^2-1+y)+1)^{1+\frac{\epsilon}{2}}} \tag{97}$$

A very useful integral for 97 is given by

$$\int_0^1 dx\int_0^1 dy \frac{1}{(a(x(1-y)^2-1+y)+1)} = -\frac{2}{a}\sqrt{a^2-4a}\;\; tanh^{-1}\left(\sqrt{\frac{a}{a-4}}\right)-\frac{a-1}{a}log(1-a) \tag{98}$$

This integral is needed in order to analytically separate the divergent pieces since $C_{122'}$ is multiplied by A_2 in the solution for Eq. 6.

$$T_{2'35} \equiv \int \frac{d^nk}{(2\pi)^n}\int \frac{d^nl}{(2\pi)^n}\frac{\mu^{2\epsilon}}{l^2((l-k)^2-m^2)k^2} = \frac{m^2\eta^\epsilon\Gamma\left(\frac{\epsilon}{2}\right)\Gamma\left(-1+\epsilon\right)\Gamma^2\left(1-\frac{\epsilon}{2}\right)}{(4\pi)^4\Gamma\left(2-\frac{\epsilon}{2}\right)} \tag{99}$$

$$T_{235} \equiv \int \frac{d^nk}{(2\pi)^n}\int \frac{d^nl}{(2\pi)^n}\frac{\mu^{2\epsilon}}{(l^2-m^2)((l-k)^2-m^2)k^2} = \frac{m^2\eta^\epsilon\Gamma^2\left(\frac{\epsilon}{2}\right)\Gamma\left(-1+\epsilon\right)\Gamma\left(1-\frac{\epsilon}{2}\right)}{(4\pi)^4\Gamma\left(2-\frac{\epsilon}{2}\right)\Gamma\left(\epsilon\right)} \tag{100}$$

The reason why the following integrals cannot be given in such a simple form is the presence of the external momentum transfer q in addition to the masses. In order to extract the infinite pieces from the next integral T_{135}, we repeatedly use the following propagator identity:

$$\frac{1}{(l+q)^2-m^2} = \frac{1}{l^2-m^2} - \frac{2lq+q^2}{(l^2-m^2)((l+q)^2-m^2)} \tag{101}$$

It then follows that

$$T_{135} \equiv \int \frac{d^nk}{(2\pi)^n}\int \frac{d^nl}{(2\pi)^n}\frac{\mu^{2\epsilon}}{((l+q)^2-m^2)((l-k)^2-m^2)k^2} = T_{235} + T_a + T_b + T_c \quad , \tag{102}$$

with

$$T_a \equiv -\int \frac{d^nk}{(2\pi)^n}\int \frac{d^nl}{(2\pi)^n}\frac{\mu^{2\epsilon}(2lq+q^2)}{(l^2-m^2)^2((l-k)^2-m^2)k^2} = \frac{q^2\eta^\epsilon\Gamma\left(\frac{\epsilon}{2}\right)\Gamma\left(\epsilon\right)\Gamma\left(1-\frac{\epsilon}{2}\right)\Gamma\left(1+\frac{\epsilon}{2}\right)}{(4\pi)^4\Gamma\left(2-\frac{\epsilon}{2}\right)\Gamma\left(1+\epsilon\right)} \tag{103}$$

$$\begin{aligned} T_b \equiv & \int \frac{d^nk}{(2\pi)^n}\int \frac{d^nl}{(2\pi)^n}\frac{\mu^{2\epsilon}(2lq+q^2)^2}{(l^2-m^2)^3((l-k)^2-m^2)k^2} = -\frac{4q^2\eta^\epsilon\Gamma\left(\frac{\epsilon}{2}\right)\Gamma\left(\epsilon\right)\Gamma\left(1-\frac{\epsilon}{2}\right)\Gamma\left(1+\frac{\epsilon}{2}\right)}{n(4\pi)^4\Gamma\left(2-\frac{\epsilon}{2}\right)\Gamma\left(1+\epsilon\right)} \\ & + \frac{q^2\left(\frac{4}{n}+\frac{q^2}{m^2}\right)\eta^\epsilon\Gamma\left(\frac{\epsilon}{2}\right)\Gamma\left(1+\epsilon\right)\Gamma\left(1-\frac{\epsilon}{2}\right)\Gamma\left(2+\frac{\epsilon}{2}\right)}{2(4\pi)^4\Gamma\left(2-\frac{\epsilon}{2}\right)\Gamma\left(2+\epsilon\right)} \end{aligned} \tag{104}$$

In passing we note that

$$T_{2235} = -\frac{1}{q^2}T_a \tag{105}$$

The last term T_c has only a simple pole in ϵ which is, however, buried in the Feynman parameter integration. This is a quite common problem that arises because of the Γ-factors in Eqs. 82 and 83. We take "u" to be that Feynman parameter and for our purposes it suffices to write the following identity:

$$\int_0^1 du(1-u)^{\frac{\epsilon}{2}-1}f(u) = \frac{2}{\epsilon}f(1) + \int_0^1 du(1-u)^{\frac{\epsilon}{2}-1}\left(f(u)-f(1)\right) \tag{106}$$

The respective terms for $T_c \equiv -\int \frac{d^nk}{(2\pi)^n}\int \frac{d^nl}{(2\pi)^n}\frac{\mu^{2\epsilon}(2lq+q^2)^3}{(l^2-m^2)^3((l+q)^2-m^2)((l-k)^2-m^2)k^2}$ are:

$$f(u) \equiv \int_0^1 dx \int_0^1 dv \frac{q^2 \eta^\epsilon u^3 v^2}{2(4\pi)^4 x^{\frac{\epsilon}{2}} \widetilde{\alpha}^{4+\frac{\epsilon}{2}}} \left(\frac{q^4}{m^4} \frac{1 - 8\frac{u^3(1-v)^3}{\widetilde{\alpha}^3} + 12\frac{u^2(1-v)^2}{\widetilde{\alpha}^2} - 6\frac{u(1-v)}{\widetilde{\alpha}}}{\widetilde{\Delta}^{2+\epsilon}} \Gamma(2+\epsilon) \right.$$
$$\left. - \frac{q^2}{m^2} \frac{6 - 12\frac{u(1-v)}{\widetilde{\alpha}}}{\widetilde{\Delta}^{1+\epsilon}} \Gamma(1+\epsilon) \right) \tag{107}$$

and thus

$$f(1) \equiv \int_0^1 dx \int_0^1 dv \frac{q^2 \eta^\epsilon v^2}{2(4\pi)^4 x^{\frac{\epsilon}{2}}} \left(\frac{q^4}{m^4} \frac{1 - 8(1-v)^3 + 12(1-v)^2 - 6(1-v)}{\left(-\frac{q^2}{m^2} v(1-v) + 1\right)^{2+\epsilon}} \Gamma(2+\epsilon) \right.$$
$$\left. - \frac{q^2}{m^2} \frac{6 - 12(1-v)}{\left(-\frac{q^2}{m^2} v(1-v) + 1\right)^{1+\epsilon}} \Gamma(1+\epsilon) \right) \tag{108}$$

Although this result for T_{135} is correct, it is numerically unstable in the massless limit because of terms of order $\frac{q^2}{m^2}$ which have to cancel as $m^2 \longrightarrow 0$. A way out of this calamity as well as a very good check on the correctness of our result for this integral is to use the propagator identity 101 for $\frac{1}{(k+q)^2}$ instead after shifting the loop momenta. This yields

$$T_{135} = T_{235} - q^2 T_{2345} - << \frac{2kq}{[2][3][4][5]} >> \tag{109}$$

The result for T_{2345} is given below and the last term in the equation can easily be found to be $2q^2 \frac{u(1-v)}{\alpha}$ times the expressions for the scalar integral. This term just stems from the momentum shift $k \longrightarrow k' - q\frac{u(1-v)}{\alpha}$. Numerically, away from the singularity at $m = 0$, both solutions agree.

In similar ways we treat the following more complicated integrals, always calling "u" the Feynman parameter that contains an additional divergence if $f(u)$-terms are quoted. The desired value for the respective integrals are understood to follow from an expansion in ϵ of Eq. 106. For

$$T_{2345} \equiv \int \frac{d^n k}{(2\pi)^n} \int \frac{d^n l}{(2\pi)^n} \frac{\mu^{2\epsilon}}{(l^2 - m^2)((l-k)^2 - m^2)(k+q)^2 k^2} \tag{110}$$

we get

$$f(u) \equiv -\int_0^1 dx \int_0^1 dv \frac{\eta^\epsilon \Gamma(\epsilon) u}{(4\pi)^4 \alpha^{2+\frac{\epsilon}{2}} \Delta^\epsilon}, \quad f(1) \equiv -\int_0^1 dv \frac{\eta^\epsilon \Gamma(\epsilon)}{(4\pi)^4 (-\frac{q^2}{m^2} v(1-v))^\epsilon} \tag{111}$$

Similarly,

$$T_{1235} \equiv \int \frac{d^n k}{(2\pi)^n} \int \frac{d^n l}{(2\pi)^n} \frac{\mu^{2\epsilon}}{((l+q)^2-m^2)(l^2-m^2)((l-k)^2-m^2)k^2} \tag{112}$$

with

$$f(u) \equiv -\int_0^1 dx \int_0^1 dv \frac{\eta^\epsilon \Gamma(\epsilon) u}{(4\pi)^4 x^{\frac{\epsilon}{2}} \widetilde{\alpha}^{2+\frac{\epsilon}{2}} \widetilde{\Delta}^\epsilon} \ , \quad f(1) \equiv -\int_0^1 dx \int_0^1 dv \frac{\eta^\epsilon \Gamma(\epsilon)}{(4\pi)^4 x^{\frac{\epsilon}{2}} (-\frac{q^2}{m^2} v(1-v)+1)^\epsilon} \tag{113}$$

For

$$T_{12'35} \equiv \int \frac{d^n k}{(2\pi)^n} \int \frac{d^n l}{(2\pi)^n} \frac{\mu^{2\epsilon}}{((l+q)^2-m^2) l^2 ((l-k)^2-m^2)k^2} \tag{114}$$

we find

$$f(u) \equiv -\int_0^1 dx \int_0^1 dv \frac{\eta^\epsilon \Gamma(\epsilon) u}{(4\pi)^4 x^{\frac{\epsilon}{2}} \widetilde{\alpha}^{2+\frac{\epsilon}{2}} \widetilde{\Delta'}^\epsilon} \ , \quad f(1) \equiv -\int_0^1 dx \int_0^1 dv \frac{\eta^\epsilon \Gamma(\epsilon)}{(4\pi)^4 x^{\frac{\epsilon}{2}} (-\frac{q^2}{m^2} v(1-v)+1-v)^\epsilon} \tag{115}$$

The infra-red finite integral

$$I_{2455} \equiv -\int \frac{d^n k}{(2\pi)^n} \int \frac{d^n l}{(2\pi)^n} \frac{\mu^{2\epsilon}(k^2+2kq)}{(l^2-m^2)(k+q)^2 k^4} \tag{116}$$

is a product of two one loop functions which are given by

$$A_2 \equiv -\frac{i m^2 \eta^{\frac{\epsilon}{2}} \Gamma\left(-1+\frac{\epsilon}{2}\right)}{(4\pi)^2} \tag{117}$$

$$I_{455} \equiv -\int_0^1 du \frac{i\zeta^{\frac{\epsilon}{2}}}{(4\pi)^2} \left(\frac{n}{2(u(1-u))^{\frac{\epsilon}{2}}} \Gamma\left(\frac{\epsilon}{2}\right) - \frac{(1-u)(1+u)}{(u(1-u))^{1+\frac{\epsilon}{2}}} \Gamma\left(1+\frac{\epsilon}{2}\right) \right) \tag{118}$$

and in dimensional regularization we have $I_{2455} = A_2 I_{455} = q^2 A_2 C_{455}$, where $A\&C$ denote the respective one loop scalar integrals. For the infra-red finite combination

$$I_{23455} \equiv q^2 T_{23455} - T_{2355} = -\int \frac{d^n k}{(2\pi)^n} \int \frac{d^n l}{(2\pi)^n} \frac{\mu^{2\epsilon}(k^2+2kq)}{(l^2-m^2)((l-k)^2-m^2)(k+q)^2 k^4} \tag{119}$$

we get two "$f(u)$" terms, distinguished below by capital (containing double pole terms) and lower case (with only simple poles) letters:

$$F(u) \equiv \int_0^1 dx \int_0^1 dv \frac{n\eta^\epsilon \Gamma(\epsilon) u^2 v}{2(4\pi)^4 \alpha^{3+\frac{\epsilon}{2}} \Delta^\epsilon} \ , \quad F(1) \equiv \int_0^1 dv \frac{n\eta^\epsilon \Gamma(\epsilon) v}{2(4\pi)^4 (-\frac{q^2}{m^2} v(1-v))^\epsilon} \tag{120}$$

$$f(u) \equiv \int_0^1 dx \int_0^1 dv A \frac{\eta^\epsilon \Gamma(1+\epsilon) u^2 v}{(4\pi)^4 \alpha^{3+\frac{\epsilon}{2}} \Delta^{1+\epsilon}} , \quad f(1) \equiv -\int_0^1 dv \frac{(1+v)\eta^\epsilon \Gamma(1+\epsilon)}{(4\pi)^4 (-\frac{q^2}{m^2} v(1-v))^\epsilon} \tag{121}$$

$$A \equiv -\frac{q^2}{m^2} \left(\frac{u^2(1-v)^2}{\alpha^2} - 2\frac{u(1-v)}{\alpha} \right) \tag{122}$$

For

$$T_{12235} \equiv \int \frac{d^n k}{(2\pi)^n} \int \frac{d^n l}{(2\pi)^n} \frac{\mu^{2\epsilon}}{((l+q)^2 - m^2)(l^2-m^2)^2((l-k)^2-m^2)k^2} \tag{123}$$

we find

$$f(u) \equiv \int_0^1 dx \int_0^1 dv \frac{\eta^\epsilon \Gamma(1+\epsilon) u^2 v}{(4\pi)^4 x^{\frac{\epsilon}{2}} \widetilde{\alpha}^{3+\frac{\epsilon}{2}} \widetilde{\Delta}^{1+\epsilon}} , \quad f(1) \equiv \int_0^1 dx \int_0^1 dv \frac{\eta^\epsilon \Gamma(1+\epsilon) v}{(4\pi)^4 x^{\frac{\epsilon}{2}} (-\frac{q^2}{m^2} v(1-v)+1)^{1+\epsilon}} \tag{124}$$

The completely finite integral $T_{12345} \equiv \int \frac{d^n k}{(2\pi)^n} \int \frac{d^n l}{(2\pi)^n} \frac{\mu^{2\epsilon}}{(l^2-m^2)((l+q)^2-m^2)((l-k)^2-m^2)(k+q)^2 k^2}$ is given by:

$$T_{12345} = \int_0^1 dx \int_0^1 dy \int_0^1 du \int_0^1 dv \frac{\eta^\epsilon \Gamma(1+\epsilon)}{m^2 (4\pi)^4} \frac{x u (1-u)^{\frac{\epsilon}{2}}}{\alpha^{3+\frac{\epsilon}{2}} \left(\frac{q^2}{m^2} \left(\frac{\sigma^2}{\alpha^2} - \frac{\rho}{\alpha} \right) + \frac{\widetilde{\alpha}}{\alpha} \right)^{1+\epsilon}} \tag{125}$$

ϵ can of course be set to zero in the above expression and we use the following abbreviations:

$$\sigma \equiv u(1-v) + (1-u)(1-y)x(1-x) \tag{126}$$

$$\rho \equiv u(1-v) + (1-u)(x(1-y) - x^2(1-y)^2) \tag{127}$$

For the "Abelian" gluon self energy graph $\mathcal{M}_{gse_4}$ we need another completely finite integral with five denominators, namely $T^A_{12345} \equiv \int \frac{d^n k}{(2\pi)^n} \int \frac{d^n l}{(2\pi)^n} \frac{\mu^{2\epsilon}}{(l^2-m^2)((l+q)^2-m^2)(l-k)^2((k+q)^2-m^2)(k^2-m^2)}$. Here we find

$$T^A_{12345} = \int_0^1 dx \int_0^1 dy \int_0^1 du \int_0^1 dv \frac{\eta^\epsilon \Gamma(1+\epsilon)}{m^2 (4\pi)^4} \frac{x u (1-u)^{\frac{\epsilon}{2}}}{\alpha^{3+\frac{\epsilon}{2}} \left(\frac{q^2}{m^2} \left(\frac{\sigma^2}{\alpha^2} - \frac{\rho}{\alpha} \right) + \frac{x(1-u)}{\alpha} \right)^{1+\epsilon}} \tag{128}$$

Again, we can savely set ϵ to zero like above. The following integrals are needed for the diagrams where we integrated out the fermion loop first, with $\pi(k^2, m^2)$ taken from Eq. 26:

$$\int \frac{d^n k}{(2\pi)^n} \frac{\mu^\epsilon \pi(k^2,m^2)}{k^2} = \int_0^1 dx \int_0^1 du \frac{m^2 \Gamma(-1+\epsilon) x(1-x)(1-u)^{-\frac{\epsilon}{2}} \eta^\epsilon}{32\pi^4 \alpha^{2-\frac{\epsilon}{2}}} \tag{129}$$

$$\int \frac{d^n k}{(2\pi)^n} \frac{\mu^\epsilon \pi(k^2,m^2)}{(k+q)^2} = \int_0^1 dx \int_0^1 du \frac{m^2 \Gamma(-1+\epsilon) x(1-x)(1-u)^{-\frac{\epsilon}{2}} \eta^\epsilon \left(-\frac{q^2}{m^2} \frac{ux(1-x)}{\alpha} + 1 \right)^{1-\epsilon}}{32\pi^4 \alpha^{2-\frac{\epsilon}{2}}} \tag{130}$$

$$\int \frac{d^n k}{(2\pi)^n} \frac{2kq\mu^\epsilon \pi(k^2,m^2)}{(k+q)^2} = \int_0^1 dx \int_0^1 du \frac{-q^2 m^2 \Gamma(-1+\epsilon) x(1-x) u (1-u)^{-\frac{\epsilon}{2}} \eta^\epsilon \left(-\frac{q^2}{m^2} \frac{ux(1-x)}{\alpha} + 1 \right)^{1-\epsilon}}{16\pi^4 \alpha^{3-\frac{\epsilon}{2}}} \tag{131}$$

Below we split again into $f(u)$ and $f(1)$ terms. For

$$\int \frac{d^n k}{(2\pi)^n} \frac{\mu^\epsilon \pi(k^2, m^2)}{(k+q)^2 k^2} \tag{132}$$

we find:

$$\begin{aligned} f(u) &= -\int_0^1 dx \int_0^1 dv \frac{\Gamma(\epsilon)\, ux(1-x)\eta^\epsilon}{32\pi^4 \alpha^{2+\frac{\epsilon}{2}} \Delta^\epsilon} & (133) \\ f(1) &= -\int_0^1 dx \int_0^1 dv \frac{\Gamma(\epsilon)\, x(1-x)\eta^\epsilon}{32\pi^4 \left(\frac{-q^2 v(1-v)}{m^2}\right)^\epsilon} & (134) \end{aligned}$$

For

$$\int \frac{d^n k}{(2\pi)^n} \frac{(k^2+2kq)\mu^\epsilon \pi(k^2, m^2)}{(k+q)^2 k^4} \tag{135}$$

there are two contributions corresponding to terms with double poles (F) and only single poles (f):

$$\begin{aligned} F(u) &\equiv -\int_0^1 dx \int_0^1 dv \frac{\Gamma(\epsilon)\, nu^2 vx(1-x)\eta^\epsilon}{64\pi^4 \alpha^{3+\frac{\epsilon}{2}} \Delta^\epsilon} & (136) \\ F(1) &= -\int_0^1 dx \int_0^1 dv \frac{\Gamma(\epsilon)\, nvx(1-x)\eta^\epsilon}{64\pi^4 \left(\frac{-q^2 v(1-v)}{m^2}\right)^\epsilon} & (137) \\ f(u) &\equiv \int_0^1 dx \int_0^1 dv \frac{q^2 \Gamma(1+\epsilon)\, u^2 vx(1-x)\eta^\epsilon \left(\frac{u^2(1-v)^2}{\alpha^2} - 2\frac{u(1-v)}{\alpha}\right)}{32 m^2 \pi^4 \alpha^{3+\frac{\epsilon}{2}} \Delta^{1+\epsilon}} & (138) \\ f(1) &= \int_0^1 dx \int_0^1 dv \frac{\Gamma(1+\epsilon)\,(1+v)x(1-x)\eta^\epsilon}{32\pi^4 \left(\frac{-q^2 v(1-v)}{m^2}\right)^\epsilon} & (139) \end{aligned}$$

B.1 Two Loop Integrals with Gluon Mass

In this appendix we give details about the evaluation of the IR-divergent integrals of section 3.1. The contributions containing heavy quark propagator terms were regulated using a gluon mass regulator and lead to the following general integral over k_0:

$$I_{k_0} \equiv \int_{-\infty}^{\infty} \frac{dk_0}{2\pi} \frac{1}{(k_0 + i\varepsilon)^2 (-k_0^2 + \mathbf{k}^2 + M^2 - i\varepsilon)^\beta} \tag{140}$$

The general power in integral 140 leads to a branch cut along the real axis for all those values for which $k_0^2 \geq \mathbf{k}^2 + M^2$. Including the $i\varepsilon$-prescription as indicated in 140, we choose a path in the complex plane around the branch cut in the upper half of the plane and find the following solution:

$$
\begin{aligned}
I_{k_0} &= -2\,i\,sin\,(\beta\pi)\int_{\sqrt{\mathbf{k}^2+M^2}}^{\infty}\frac{dk_0}{2\pi}\frac{1}{k_0^2|-k_0^2+\mathbf{k}^2+M^2|^{\beta}} \\
&= -2\,i\,sin\,(\beta\pi)\,\frac{\Gamma\,(1-\beta)\,\Gamma\left(\frac{1}{2}+\beta\right)}{2\pi^{\frac{3}{2}}(\mathbf{k}^2+M^2)^{\frac{1}{2}+\beta}} \qquad (141)
\end{aligned}
$$

The remaining Euclidean integral can then be performed easily. In the case of the crossed ladder diagram $\mathcal{M}_{cl}$ we find in this manner again a divergence which is hidden in Feynman parameters. This can be handled by splitting into $f(u)$ and $f(1)$ terms as above. For

$$
\int\frac{d^nk}{(2\pi)^n}\frac{\mu^{\epsilon}\pi(k^2,m^2)}{(k_0+i\varepsilon)^2(k^2-\lambda^2+i\varepsilon)((k+q)^2-\lambda^2+i\varepsilon)} \qquad (142)
$$

we find

$$
f(u) = 16\,sin\left(\frac{\epsilon}{2}\pi\right)\frac{\Gamma\left(-1-\frac{\epsilon}{2}\right)\Gamma\,(1+\epsilon)\,\Gamma\left(2+\frac{\epsilon}{2}\right)\eta^{\epsilon}}{(4\pi)^4\pi\;m^2}\int_0^1 dx\int_0^1 dv\frac{x(1-x)\;u}{\alpha^{2+\frac{\epsilon}{2}}\left(\Delta+\frac{\lambda^2}{m^2}u\right)^{1+\epsilon}} \qquad (143)
$$

$$
f(1) = 16\,sin\left(\frac{\epsilon}{2}\pi\right)\frac{\Gamma\left(-1-\frac{\epsilon}{2}\right)\Gamma\,(1+\epsilon)\,\Gamma\left(2+\frac{\epsilon}{2}\right)\eta^{\epsilon}}{(4\pi)^4\pi\;m^2}\int_0^1 dx\int_0^1 dv\frac{x(1-x)}{\left(\frac{-q^2}{m^2}v(1-v)+\frac{\lambda^2}{m^2}\right)^{1+\epsilon}} \qquad (144)
$$

The vertex correction graph $\mathcal{M}_{vc_3}$ and the integral occurring in the onle-loop verex correction term $\mathcal{M}_{olvc}$ can be calculated analogously. Here we have

$$
\int\frac{d^nk}{(2\pi)^n}\frac{\mu^{\epsilon}\pi(k^2,m^2)}{(k_0+i\varepsilon)^2(k^2-\lambda^2+i\varepsilon)} \qquad (145)
$$

with the corresponding solutions

$$
f(u) = -16\,sin\left(\frac{\epsilon}{2}\pi\right)\frac{\Gamma\left(-\frac{\epsilon}{2}\right)\Gamma\,(\epsilon)\,\Gamma\left(1+\frac{\epsilon}{2}\right)\eta^{\epsilon}}{(4\pi)^4\pi\;q^2}\int_0^1 dx\frac{x(1-x)}{\alpha^{1+\frac{\epsilon}{2}}\left(1-u+\frac{\lambda^2}{m^2}u\right)^{\epsilon}} \qquad (146)
$$

$$
f(1) = -\frac{8}{3}\,sin\left(\frac{\epsilon}{2}\pi\right)\frac{\Gamma\left(-\frac{\epsilon}{2}\right)\Gamma\,(\epsilon)\,\Gamma\left(1+\frac{\epsilon}{2}\right)\eta^{\epsilon}}{(4\pi)^4\pi\;q^2}\left(\frac{m^2}{\lambda^2}\right)^{\epsilon} \qquad (147)
$$

Acknowledgments

The author would like to thank S.J. Brodsky for very valuable discussions in the early stages of the paper. G. Buchalla and M. Peter are greatfully acknowledged for helpful communications on technical aspects of this work. Thanks also go to T. Hurth, M. Wuesthoff, M. Heyssler and J. Rathsman for constructive conversations on several matters.

References

[1] A. Billoire. *Phys. Lett.*, B 92:343, 1980.

[2] A.H. Hoang, M. Jezabek, J. H. Kühn, T. Teubner. *Phys. Lett.*, B 338:330, 1994.

[3] B.A. Kniehl. *Nucl. Phys.*, B 347:86, 1990.

[4] Collins. Renormalization. *Cambridge University Press*, 1984.

[5] E. De Rafael, J.L. Rosner. *Annals of Physics*, 82:369, 1973.

[6] F.L.Feinberg. *Phys. Rev. D*, 17:2639, 1978.

[7] G. Buchalla, A.J. Buras, M.E. Lautenbacher. *Rev. Mod. Phys.*, D 47:1125, 1994.

[8] G. Källen, A. Sabry. *K. Dan. Vidensk. Selsk. Mat.-Fys. Medd.*, 17:29, 1955.

[9] G. Rodrigo, A. Santamaria. *Phys. Lett.*, B 313:441, 1993.

[10] G. Weiglein, R. Scharf, M. Boehm. *Nucl. Phys.*, B 416:606, 1994.

[11] G.Passarino, M.Veltman. *Nuclear Physics*, B160:151, 1979.

[12] Itzykson, Zuber. Quantum field theory. *McGraw-Hill Book Company*, 1980.

[13] J.A.M.Vermaseren. The symbolic manipulation language form, version 1, available via anonymous ftp from nikhefh.nikhef.nl. 1990.

[14] K.G. Chetyrkin, B.A. Kniehl, M. Steinhauser. *Phys. Rev. Lett.*, 79:2184, 1997.

[15] L. Hall. *Nucl. Phys.*, B 178:75, 1981.

[16] L. Susskind. Coars grained qcd. *R. Balien, C.H. Llewellyn Smith (eds.)*, North Holland, Amsterdam, 1977.

[17] L.H.Ryder. Quantum field theory. *Cambridge University Press*, 1985.

[18] M. Beneke, V.A. Smirnov. *hep-ph/9711391*, 1997.

[19] M. Neubert. *Phys. Rept.*, 245:259, 1994.

[20] M. Peter. private communications.

[21] M. Peter. *Nucl. Phys.*, B 501:471, 1997.

[22] M. Peter. *Phys. Rev. Lett.*, 78:602, 1997.

[23] M.E. Peskin, D.V. Shroeder. Introduction to quantum field theory. *Addison-Wesley Publishing Company, Inc.*, 1995.

[24] O.V. Tarasov. *Nucl. Phys.*, B 502:455, 1997.

[25] P. Lepage. Vegas, a monte carlo integrater. *freely available*, (c) 1995, Cornell University.

[26] Pascual, Tarrach. Qcd: Renormalization for the practitioner. *Springer-Verlag*, 1984.

[27] R. Barbieri, E. Remiddi. *Nouvo Cim.*, A 13:99, 1973.

[28] S. Weinberg. *Phys. Lett.*, B 91:51, 1980.

[29] S.J. Brodsky, G. P. Lepage, P. B. Mackenzie. *Phys. Rev. D*, 28:228, 1983.

[30] S.J. Brodsky, M. Gill, M. Melles, J. Rathsman. *SLAC-PUB 7157; HEP-ph/9801330, submitted to Phys. Rev. D.*, 1998.

[31] S.L.Adler, R.F.Dashen. Current algebras. *W.A. Benjamin, Inc.*, 1968.

[32] S.Pokorski. Gauge field theories. *Cambridge University Press*, 1987.

[33] T. Appelquist, J. Carazzone. *Phys. Rev.*, D 11:2856, 1975.

[34] T. Appelquist, M. Dine, I.J. Muzinich. *Phys. Lett.*, B 69:231, 1977.

[35] T. Appelquist, M. Dine, I.J. Muzinich. *Phys. Rev.*, D 17:2074, 1978.

[36] T. Muta. An introduction to perturbative methods in gauge theories. *World Scientific Publishing Company, Inc.*, 1987.

[37] W. Bernreuther. *Ann. Phys.*, 151:127, 1983.

[38] W. Bernreuther. *Z. Phys.*, C 20:331, 1983.

[39] W. Bernreuther, W. Wetzel. *Nucl. Phys.*, B 197:228, 1982.

[40] W. Wetzel. *Nucl. Phys.*, B 196:259, 1982.

[41] W.Fischler. *Nucl. Phys. B*, 129:157, 1977.

[42] W.J. Marciano. *Phys. Rev.*, D 29:580, 1984.